ANALYTICAL MODEL FOR FORCE PREDICTION WHEN MACHINING METAL MATRIX COMPOSITES

By

Snahungshu Sikder

A thesis submitted in conformity with the requirements
for the degree of Master of Applied Science

In

Faculty of Engineering and Applied Science

University of Ontario Institute of Technology

ABSTRACT

Metal Matrix Composites (MMC) offer several thermo-mechanical advantages over standard materials and alloys which make them better candidates in different applications. Their light weight, high stiffness, and strength have attracted several industries such as automotive, aerospace, and defence for their wide range of products. However, the wide spread application of Meal Matrix Composites is still a challenge for industry. The hard and abrasive nature of the reinforcement particles is responsible for rapid tool wear and high machining costs. Fracture and debonding of the abrasive reinforcement particles are the considerable damage modes that directly influence the tool performance. It is very important to find highly effective way to machine MMCs. So, it is important to predict forces when machining Metal Matrix Composites because this will help to choose perfect tools for machining and ultimately save both money and time. This research presents an analytical force model for predicting the forces generated during machining of Metal Matrix Composites. In estimating the generated forces, several aspects of cutting mechanics were considered including: shearing force, ploughing force, and particle fracture force. Chip formation force was obtained by classical orthogonal metal cutting mechanics and the Johnson-Cook Equation. The ploughing force was formulated while the fracture force was calculated from the slip line field theory and the Griffith theory of failure. The predicted results were compared with previously measured data. The results showed very good agreement between the theoretically predicted and experimentally measured cutting forces.

ACKNOWLEDGEMENTS

I would like to express my earnest gratitude to my thesis supervisor Dr. H. A. Kishawy for his able guidance, encouragement and endless support throughout the courses and thesis. I also truly appreciate his helpful advice and time.

Thanks go to members of the thesis committee Dr. Zhang, Dr. Reddy, and Dr. Barari for their time. I wish to thank the Natural Sciences and Engineering Research Council of Canada for its financial support. Special thanks to all my colleagues in the Machining Research Lab: Lei, Ali, and Grant.

Last, but not least, I thank my parents: Mr. Mihir Kumar Sikder, and Mrs. Shikha Saha for their unconditional support and loving encouragement throughout my life. I would also like to thank my aunt Mrs. Shubhra Saha for her loving support, care and guidance without which it would have been impossible for me to reach this far. I wish to thank my dear sister Jhinuk and cousins Anik, Ishita, Showvik, and Avik for their love and strong support in all my endeavours.

Table of Contents

TABLE OF FIGURES

LIST OF TABLES

NOMENCLATURE

A, B, n, m	Johnson-Cook equation constants
$\alpha_R \alpha_M$	The thermal expansion coefficients of reinforcements and matrix
a	Un-deformed chip thickness
b	Width of cut
β	Friction angle
Co	Kronenberg constant
δ	The angle between the resultant force and cutting direction
E	Equivalent shear strain.
$\dot{\varepsilon}$	Dimensionless shear rate
F_{N1}	Normal force on individual abrasive particle.
$F, F_s, F_f, F_n, F_c, F_T$	Forces (Shear, Friction, Normal, Cutting, Thrust direction)
$G_M G_R$	Shear modules of the matrix metal and reinforced particles
H_t	Hardness of tools
φ	Shear angle
K	Shear flow stress
K_{MMC}, K_M, K_R	The bulk module of composites, matrix metal and reinforced particles
K_s	Unit force
h	Specific heat of material
l	Equivalent cutting length

σ	Fracture stress
N_p	Total number of reinforcement particles at tool–chip interface
θ_a	Approach angle
θ_p	Apex angle
∂_{Po}	Critical value of relative penetration
q	The fraction of the particle involved in two body abrasion
r_n, r_e	Nose and edge radius
r_c	Chip thickness ratio
r_{groove}	Depth of groove formed on tool face due to abrasion wear
$\sigma_{y(tool)}$	Yield strength of tool material
T, T_r, T_m	Cutting, Room and Melting temperature
τ_s	Shear stress
τ_{so}	Shear stress of the material under zero compressive stress
γ	Rake angle
U	The fracture energy per particle
V	Cutting velocity
Vs	Velocity along shear plane
Vc	Chip velocity
W	Thermal conductivity of material
Y_{MMC}, Y_R, Y_M	Young's modulus of MMC, Reinforcement and Matrix

CHAPTER 1

INTRODUCTION

1.1 Background

Manufacturing is the backbone of any modern industrialized economy. In manufacturing material removal or machining is one of the oldest and most indispensable processes for shaping components. Machining process with its intrinsic versatility and associated precision machine tools capable of being driven by computers has been responsible for recent industrial advancements.

The main objective of machining is to produce a product of required shape and dimension with specific quality and surface finish. The metal cutting process is accompanied by deformation in the form of compression, tension which involves a considerable amount of heat transfer through the tiny area around the tool tip [1].

The growth of a manufacturing based economy largely depends on the development of various machining operations. The driving force behind this development is the ability to

make parts of different shapes with high quality and precision both faster and at lower cost. In view of its economic importance, complexity of the process, and to develop new cutting equipments, techniques, or processes, researchers have continuously expressed their desire in understanding the principals of cutting mechanisms. Machining is challenged by the discovery of new generation of materials such as alloys, composites which are often difficult to cut. Comprehensive understanding of cutting mechanics can help to develop new techniques, tools and machining processes.

A Metal Matrix Composite (MMC) is a composite material in which one constituent is a metal or alloy forming at least one percolating network, while the other constituent is embedded in this metal matrix and usually serves as reinforcement [2]. The reinforcement in MMC could be particulate, fibers, or whiskers with volume fraction ranging from a few percent to 40%. Compared to other materials, MMCs generally have much higher strength, stiffness and wear resistance as well as lower weight and thermal coefficient of expansion. In some cases they have lower lifecycle costs than other conventional materials [3].

MMCs have been available for quite some time but have only been recognized by industries in the 2nd half of the twentieth century [2]. Increased interest in utilizing MMCs has motivated researchers to develop different types of MMCs. Over the last three decades, researchers on MMCs have provided not only new types of MMCs but also characterized them in terms of physical, thermo-mechanical, tribological, and machining

properties. On the other hand, considerable research has been done on production techniques, processing, interface, and micro-mechanic behaviour.

It is interesting to note that research on machining of MMCs was begun during the 1980s. Most of these studies were based on Aluminum matrix composite materials. These studies focused on the machinability, specifically the tool life and the optimization of cutting tool performance. According to Pramanik *et al.* [4] the research can be divided in three categories

1. Experimental studies that compare different tools and/or coating for Machining MMCs.
2. Empirical and numerical studies related to tool life.
3. Experimental studies on performance of Polycrystalline Diamond (PCD) tools, machined surface and optimization of cutting parameters, tool geometry, and work piece compositions.

Only a few studies have examined cutting forces and presented models for predicting the generated forces while machining MMCs [4].

1.2 Research Scope and Objectives

MMCs are a potential substitute to conventional metals, alloys, and polymers in various applications due to their low weight and toughness. The UK Advisory Council on Science & Technology in 1992 stated that, “MMCs can be viewed either as a replacement

for existing materials, but with superior properties, or as a means of enabling radical changes in system or product design." [3] Moreover, by utilising near-net shape forming and selective reinforcement techniques MMCs can offer economically viable solutions for a wide variety of commercial applications [2].

Use of metal matrix composites as an industrial material is increasing but the cutting of MMC is extremely difficult due to the high hardness and abrasive nature of the reinforcements. During the machining the MMC, reinforcement particles are fractured and pulled out of the matrix which lead to the deterioration of the product surface quality, rapid tool wear, and increased machining costs. Moreover, premature failure of the cutting tool leads to recurrent tool changes which increases production time and cost. The focus of this work is to provide an analytical cutting force model and force characteristics during the machining of metal matrix composites. The objectives of the thesis are:

1. To review the fundamental mechanics of cutting MMCs based on identifying the different types of forces generated during machining. Those forces are then quantified using mathematical expressions which are used to develop the thermo-mechanical model for predicting cutting forces generated during machining MMCs. During the analytical model development the friction between the chip tool interface, volume fractions and average size of the particulate reinforcements are taken into account.
2. Validate the proposed thermo mechanical model for predicting cutting and thrust forces by comparing the previously measured and predicted results.

1.3 Thesis Outline

Chapter 2 describes an overview on metal matrix composites. It also includes characteristics, production processes, and applications of MMCs.

Chapter 3 contains a comprehensive literature review of publications presenting the basic terms and definitions used in metal cutting. It covers fundamental aspects of metal cutting, cutting angles, chip formation, chip-tool friction and cutting mechanics, and problems relating to the machining of MMCs.

Chapter 4 describes a "Thermo Mechanical Analytical" approach for predicting the forces generated during the machining of MMCs.

Chapter 5 presents experimental verification of the proposed model. Detailed characteristics of cutting forces and comparison between the predicted forces and experimental force are presented.

Chapter 6 presents the conclusions of the findings from the current work and suggestions for the future investigations.

CHAPTER 2

Metal Matrix Composites

2.1 Introduction

Material matrix composites have the potential to be replacements for conventional metal and alloys. MMCs are the next generation of materials with good physical, chemical, and mechanical properties. Metal matrix composites are widely used in the automobile, aerospace, and defense industry due to their high strength ratio to weight and improved thermo-mechanical properties. Figure 2.1 shows that specific strength and specific stiffness are greater than conventional alloys. MMCs have been used commercially in pistons and aluminum crank cases and disk brakes. In this chapter, a compressive overview of metal matrix composites will be presented through including types; production techniques; and effects of reinforcements, application and characteristics of MMCs.

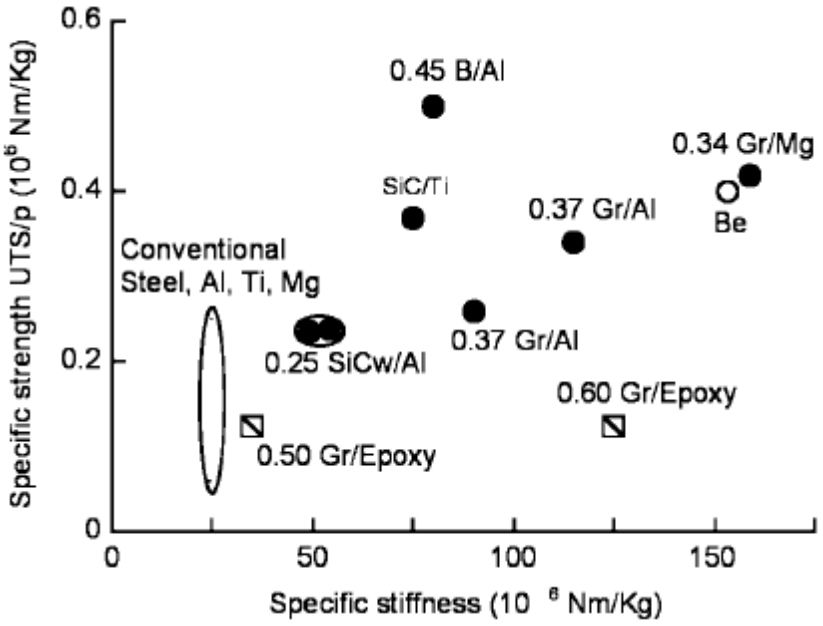

Figure 2.1: Specific strength vs. specific stiffness for various MMC materials. Number in front of the composite is the reinforcement volume fraction [5].

2.2 Metal Matrices and Reinforcements

Generally, a metal matrix composite is a material having two constituent parts; one being a metal and the other material can be a different metal or ceramic. Metal matrix composite materials are generally classified based on their physical and chemical properties. MMCs can be fall in the following groups considering reinforcements (shown in Figure 2.2):

1. Particle reinforced MMCs;
2. Whiskers or Short fiber reinforced MMCs;
3. Long fiber or continuous fiber reinforced MMCs.

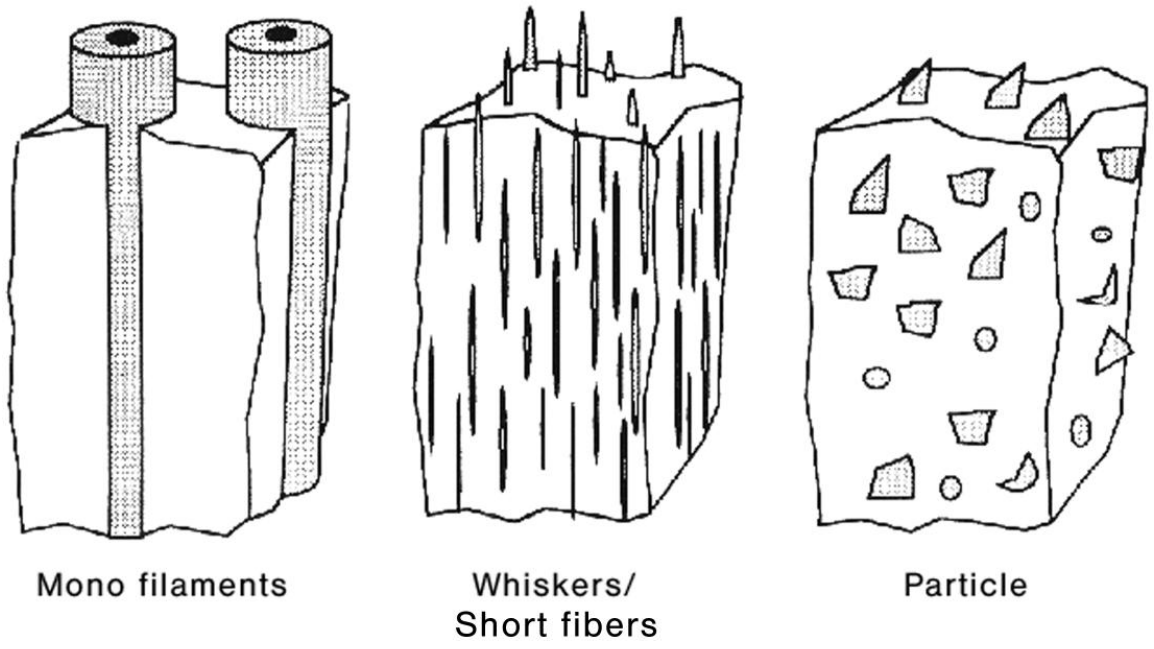

Figure 2.2: Schematic presentation of different types of MMC [6]

Reinforcement size differs from 2-200 micrometer and volume fraction varies from 5 to 40%. Figure 2.2 shows the schematic representation different types of reinforcement used in metal matrix composites. Generally matrices are based on aluminum, copper, zinc, steel, magnesium. Reinforcements used are generally silicon carbide, titanium carbide, aluminum oxide, soda ash, boron nitride, graphite. Table 2.1 shows typical types of reinforcements used in each category of reinforcement.

Table 2.1: Some Important Reinforcement of Metal Matrix Composites [2]

Type of MMCs	Reinforcements
Particle reinforced	$Al_2O_3, SiC, WC, TiC, B_4C$
Continuous fibre reinforced	$Al_2O_3, SiC, B, C, Al_2O_3 + SiO_2, Nb - Ti, Nb_3Sn, Si_3N_4$
Whiskers or Short fibre	$Al_2O_3, Al_2O_3 + SiO_2, SiC, TiB_2$

2.3 Manufacturing Methods

There are different processes for manufacturing MMC which can be divided into two categories based on the operating state of matrix metal:

1. Solid state processes;
2. Liquid state processes.

Powder metallurgical processes, diffusion bonding, and vapors deposition are the techniques that come under the solid state technique. Powder metallurgical processes generally are:

a) Pressing and sintering or forging of powder mixtures and composites;
b) Extrusion or forging of metal-powder particle mixtures [7,8];
c) Extrusion or forging of spraying compatible precursor materials [9-11].

On the other hand liquid state process includes:

a) Stir casting;
b) Gas pressure infiltration process;
c) Squeeze or pressure casting;
d) Vortex casting;
e) Injection method.

Figure 2.3 (schematic diagram) shows all the technique involved in liquid state process. Most of the particle reinforced MMCs are manufactured through liquid state process. In this thesis, the used MMCs are manufactured through this process.

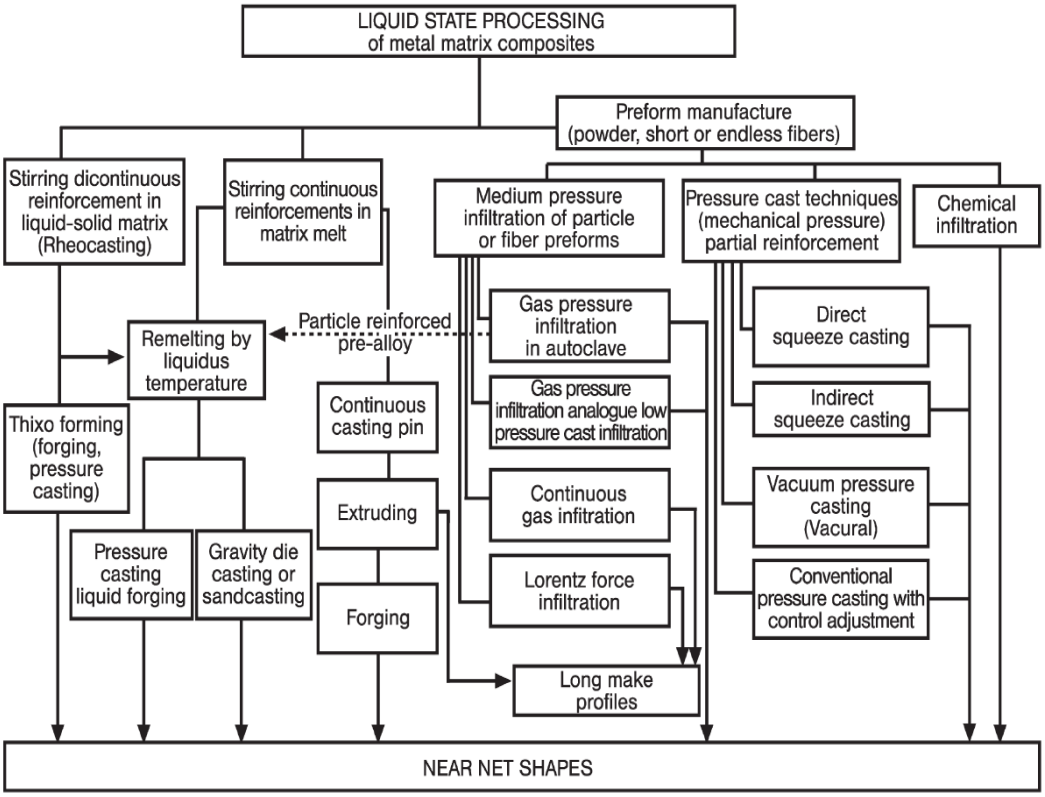

Figure 2.3: Liquid state processing of MMC [12]

The manufacturing process is often chosen based on the desired kind of quality, reinforcement materials, matrix alloy and the application of the MMC. By changing the manufacturing technique, the processing and the finishing, as well as by the form of the reinforcement components, it is possible to obtain different characteristic profiles even though the composition and amount of component involved are the same [12].

2.4 Mechanical Behaviors of MMCs

In this section, effects of reinforcements, strengthening, and cyclic fatigue will behaviour of MMCs will be discussed.

2.4.1 Effect of Reinforcement on MMC

The presence of reinforcement particles affects the behaviour of the matrix metal largely during its manufacturing, heat treatment and its subsequent use. In this section the effect of reinforcement particles on the physical properties and failure are discussed:

Young's Modulus: One of the main objectives in the development of metal matrix composite materials is to increase the modulus of elasticity. Generally, the volume fraction of the reinforcement and metal matrix is the key factor behind the change in Young's modulus. The universally used models to determine the elastic modules are the following linear and inverse mixture rules [5, 12].

Linear Mixture rule:

$$Y_{MMC} = V_P Y_R + (1 - V_P) Y_M \tag{2.1}$$

Inverse mixture rule:

$$\frac{1}{Y_{MMC}} = \frac{V_p}{Y_R} + \frac{1 - V_p}{Y_M} \tag{2.2}$$

Where, V_p represents the volume fraction and Y_{MMC}, Y_R and Y_M represents the Young's modulus of MMC, reinforce fibre, and matrix metal, respectively.

Thermal Co-efficient: Reinforcement of light metal alloys with ceramic fibers or particles causes a decrease in the thermal expansion coefficients. Simple models are available to estimate the thermal expansion coefficients with the help of the characteristics of the individual components. The model of Schapery [13] was developed to describe the influences on the thermal expansion coefficients of fibrous MMCs:

$$\alpha_{3c} = \frac{\mathrm{Y_R}\alpha_R \mathrm{V_p} + \mathrm{Y_M}\alpha_M(1-\mathrm{V_p})}{Y_{MMC}} \tag{2.3}$$

Where, α_{3c} represents the axial thermal expansion coefficients of MMC, α_R, α_M represent the thermal expansion coefficients of reinforcements and thermal expansion coefficients of matrix, respectively.

For the case of particular reinforcements Schapery [13] gives an upper and lower bound Equations are given by:

$$\alpha_C = \mathrm{V_p}\alpha_R + \left(1-\mathrm{V_p}\right)\alpha_M + \left[\frac{4\mathrm{G_M}}{K_{MMC}}\right]\left[\frac{(K_{MMC}-K_R)(\alpha_M-\alpha_R)\mathrm{V_p}}{4\mathrm{G_M}+3K_R}\right] \tag{2.4}$$

$$\alpha_C = \mathrm{V_p}\alpha_R + \left(1-\mathrm{V_p}\right)\alpha_M + \left[\frac{4\mathrm{G_R}}{K_{MMC}}\right]\left[\frac{(K_{MMC}-K_M)(\alpha_P-\alpha_M)(1-\mathrm{V_p})}{4\mathrm{G_R}+3K_M}\right] \tag{2.5}$$

Where, K_{MMC}, K_M, K_R represent the bulk moduli of composites, matrix metal and reinforced particles respectively. Again $\mathrm{G_M}, \mathrm{G_R}$ represent the shear moduli of the matrix metal and reinforced particles.

Failure Modes: Failure modes also depend on reinforcement particle size, shapes and volume fraction. Hunt *et al.* [14] and Beck *et al.* [15] examined different MMCs to determine the fracture toughness. They observed that the fracture toughness was a function of volume fraction. They reported decrease in toughness with volume fraction but from their experiments it was not clear the effect of particle size on toughness.

Thermal co-efficient mismatch between the reinforcement and metallic part of MMC is one of the main reasons for failure [16]. Thermal stress can be developed due to any temperature change both either heating or cooling. Generally metals have higher thermal expansion co-efficients than reinforcement particles. So, a large internal stress developed during heating and cooling due to the mismatch of thermal co-efficient. If, it happens in repeated manner then thermal fatigue occurs due to cyclic stress. According to Chawla and Chawla [16], it causes plastic deformation and cavitations in ductile matrix.

2.4.2 Strengthening Mechanism

Several researchers have worked on different strengthening mechanism that may occur in different metal matrix composites. Generally strengthening mechanisms can be divided into two categories. They are described below

1. Direct strengthening: Direct strengthening generally applied in continuous fiber MMCs but it can also be applied in particle reinforced MMCs too. In direct strengthening, load transferred from the matrix metal to reinforced particles which

have higher stiffness. In this way strengthening takes place by reinforcement particles absorbing most of the applied load.

2. Indirect strengthening: Indirect strengthening occurs due to change in micro structures and properties of reinforcement particles. There are different kinds of indirect strengthening of MMCs reported by various researchers. They are as follows [17]:
    a. Quench Strengthening: The large difference between in the thermal expansion between matrix metal and reinforcement results in quench strengthening in metal matrix composites.
    b. Orowan Strengthening: In this case, Orwan bypass of particles by dislocations can increase the strength of a material.
    c. Grain Strengthening: During thermo mechanical processing particular reinforcement MMC may re-crystallize. The presence of a ceramic particulate influences the nucleation rate of the matrix grains. The resulting size of the grain directly affects the yield strength of the MMC, according to the Hall-Petch effect (Grain-boundary strengthening).
    d. Sub-structure Strengthening: It has been shown that above a critical ratio of volume fraction to particle size, the material will retain a fine grain structure. In this case, the sub-structure will contribute to MMC strength through the Hall-Petch effect.
    e. Work Hardening: Generally, work hardening of MMCs is influenced by the dislocation structure formed during quenching.

2.5 Applications of MMC

Metal matrix composites are widely used in different industries due to its high strength to weight ratio and improved thermo-mechanical properties. For many years MMCs have been used in different industrial areas including

a. Aerospace;
b. Transportation;
c. Electrical and thermal;
d. Sporting and recreational products;
e. Filamentary superconducting magnets;
f. Power conduction;
g. Wear-resistant materials.

MMCs have been used in several applications as aerospace components. In aerospace industries it has been used due to its low weight, thermal expansion and conductivity, high stiffness, and strength. MMCs have been used largely in military aircrafts. Rotating blades of helicopters, doors ($Al - SiC$ MMC) are made from MMCs [2]. In different military fighter planes e.g., the ventral fin of F-16, fuel access door covers are made from MMCs. MMCs are also used in commercial aircrafts like Boeing 777. The fan-exit guide vanes of Pratt and Whitney engines are made from MMC instead of carbon/epoxy composite. Missiles wings and fines are made from MMC because of its enhanced strength, stiffness, and low weight than steel and titanium. Space structure like space shuttle and Hobble telescope are made from carbon fiber reinforced aluminum.

For the case of automotive and rail industries MMCs are commonly used in breaking system. They are also used in connecting rods, driver shafts, cylinder liners of engine, gears parts, and suspension arms [2].

Particle reinforced MMCs are used in the sports and recreational industry. Golf club shafts, heads, skating shoes, track shoe spikes, baseball shafts, horseshoes, and bi-cycle frames are also made form MMC. On the other hand, it has been used as microwave housing, carrier plates, and integrated heat sink in electronic packaging.

2.6 Summary

This chapter has described several aspects of MMC from production to the application of MMCs. The fundamental goal of this chapter was to provide an overview of MMCs as an engineering material.

CHAPTER 3

LITERATURE REVIEW

3.1 Introduction

Metal cutting and forming have been traditionally the most common manufacturing processes from the old ages. Machining processes have been here for a long time but scientific researches on machining started only during 19th century. Research has been done on several aspects of metal cutting such as chip-formation, cutting mechanics, machined surface, tool wear-life etc. Chapter 3 provides exhaustive review of literature that deals with problems encountered during metal cutting processes including chip formation and cutting forces for conventional metals and MMCs. In this chapter, an attempt has been made to describe the relevant aspects of metal cutting relevant to this work.

3.2 Theory of Metal Cutting

Metal cutting as a manufacturing process has been around for a long time but systematic research on metal cutting started during 1850s. According to Finnie [18], the early work dated back to the 1850's. This was aimed to understand the dependence of machining forces on cutting conditions, tool geometry, other process variables, and the mechanics of chip formation to the estimate power requirements from a steam engine [19]. The first work reported by Finnie [18] and Zorev [20] was carried out by Cocquilhat [21] to calculate the work required to cut a unit volume of different materials using a drilling process.

Several researchers during that time constructed crude dynamometer to measure cutting forces and conducted machining experiments. Among that group the best known was Hartig [22] whose book published in 1873 was the standard reference for many years [18]. Other researchers (e.g. Time [23], Tresca [24], and Mallock [25]) studied mechanism of chip formation. Tresca [24] proposed that chip formation was a shearing process. He also reported that the chips were formed due to the compression ahead of the tool tip. This compression caused shear failure parallel to work surface and sheared away the extra material as chips from the work surface. This theory was later verified by Mallock [25].

Best known as a founder of scientific measurement, Frederick W. Taylor was first to implement management theory in the field of metal cutting [19]. Taylor specified

engineering objectives of machining as business orientated and thoroughly practical to get more, better, and cheaper work out of a machine shop [26].

A number of significant research advancements were made during the period from 1930-1960. In 1938, Ernst [27] studied the movement of the tool during metal cutting using motion picture camera and microscope. He first categorized chips into three categories: discontinuous, continuous, and continuous with built up edges (BUE). In 1938 Piispanen [28] developed his "deck of cards" model to explain formation of chips. The shear plane theory of metal cutting was developed by Ernst [27] and Merchant [29] which provided a better understanding of the cutting process. Merchant's model was quantitatively accurate for many cases. On the other hand Trigger and Chao [30], and Loewen and Shaw [31] developed an accurate steady state model to predict cutting temperature. After, the 1950s with the increase of machining speed and introduction of automation, many researchers started researching on the dynamic stability of machine tools. Since then, researchers started to work on all possible fields in machining.

Many trials were made since Merchant [29] work to predict cutting forces during machining of conventional materials based on different mechanism for different kinds of arrangements [32-36].

3.3 Mechanics of Chip Formation

Metal cutting involves the systematic removal of a layer of metal in the form of chips from a blank to give the desired dimension and shape with desired surface quality. Two

different mechanisms for metal removal exist: orthogonal cutting and oblique cutting, shown in Figure 3.1. In the orthogonal cutting, the cutting edge is perpendicular to the direction of work-tool motion. In oblique cutting, the cutting edge inclination angle is other than 90° with work-tool motion.

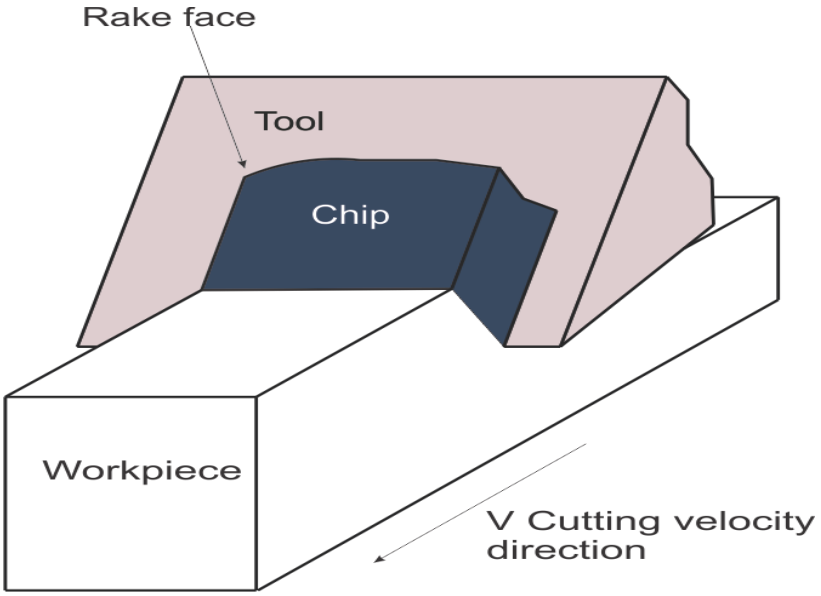

(a) Orthogonal Metal Cutting

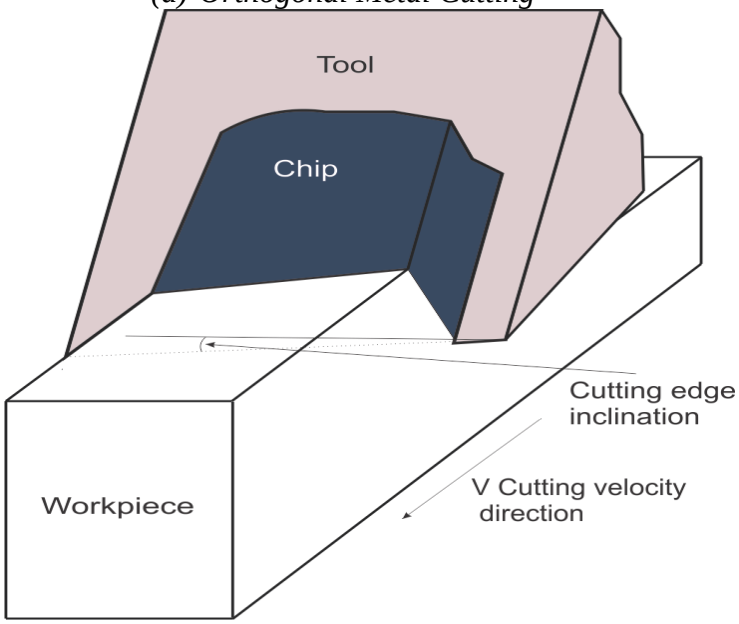

(b)Oblique Metal Cutting

Figure 3.1: Two types of basic metal cutting

During metal cutting, tools starts to penetrate the work-piece and build up a large amount of stress. Large elastic and plastic deformation take place when this stress reaches the yield strength of the material. The boundary zone between the deformed and unreformed metal is called the shear plane (Figure 3.2).

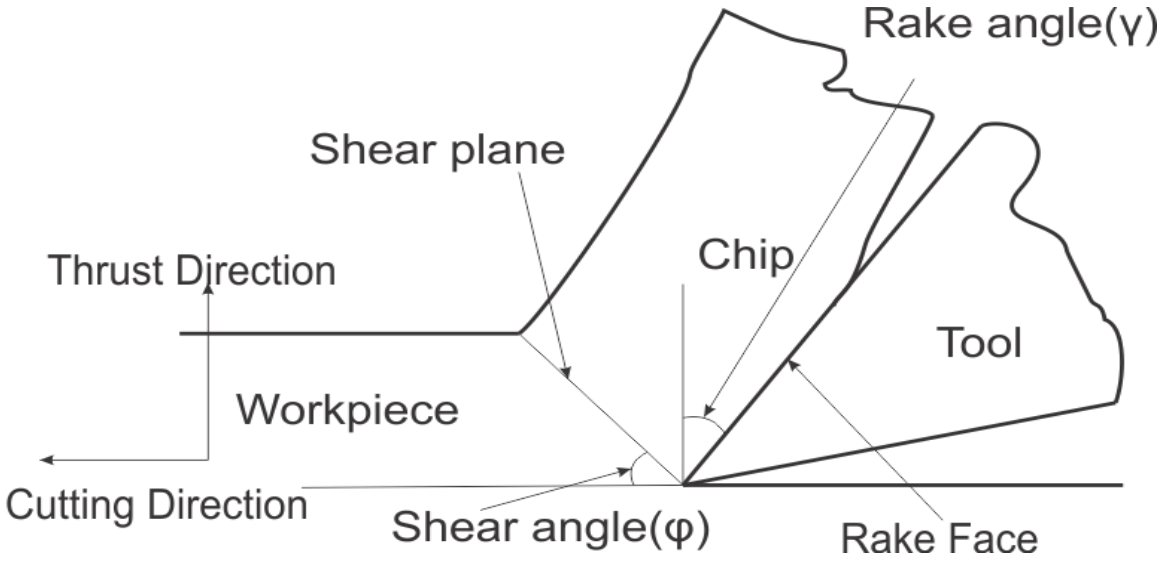

Figure 3.2: Thin shear plane

The angle between the shear plane and cutting direction is called shear angle. Deformed materials in the shear zone flow through the chip-tool interface in the form of chips. In this process considerable amount of forces are involved for the shearing process and chips flow along the tool faces. It is important to predict the forces involved in metal cutting with its' magnitude and direction. On the other hand, the geometry of the cutting tool (e.g., tool angles and different edges), cutting conditions (e.g., cutting speed, depth of cut, and feed), material flow characteristics, thermo–physical properties of the material and chip-tool interface conditions are the main factors that affect the chip formation.

Produced chips were classified into three groups by Ernst and Merchants. They are:

1. Discontinuous chips;
2. Continuous chips;
3. Continuous chip with built-up edges.

In addition to these chips there are some other types of chips including:

1. Wavy Chips;
2. Segmented Chips;
3. Saw tooth Chips.

Discontinuous chips are formed during machining of ductile materials, such as cast iron and /or when machining ductile materials at very low cutting speed in absence of cutting fluid. In this case, instead of continuous shearing, rupture occurs intermittently producing segments of chips (Figure 3.3) [37].

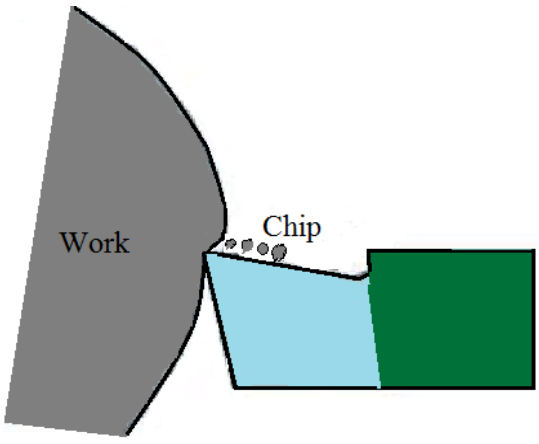

Figure 3.3: Discontinuous chip

In the case of machining soft materials with moderate cutting speeds continuous chips are formed (Figure3.4). In this chase the shear zone is well defined where the shear action takes place along the shear plane.

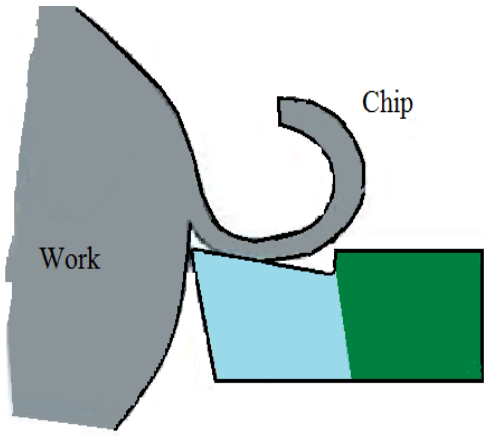

Figure 3.4: Continuous chip

As the cutting speed increases, instability in the shearing process and resistance in chip tool interface increases [38]. These instabilities cause void formation around the secondary phase particles in the work-piece material which eventually join up and form cracks. This is the main cause for partially fractured chips. Segmented chips are formed due to strain hardening of the chips at tool tip and thermal softening of chip in the secondary shear zone [39]. Again, at high cutting speed for different metals adiabatic shear occurs, which ultimately leads to saw –tooth type of chips. Adiabatic shear is due do shear localization in narrow confined zone. At high cutting speed the heat generated in the shear plane cannot dissipate causing a locally deformed shear band. Continuous chips with build up edge are formed when plastic flow in the cutting zone takes place and the resistance of relative motion between chip and tool is very high. This resistance causes temperature and pressure rise in chip tool interface. Due to the high temperature and pressure at the tool face causes a localized welding of the chip material to the tool face. As the tool advances, the welded part increases until it reaches the critical size and breaks down to form continuous chip with BUE (Figure 3.5).

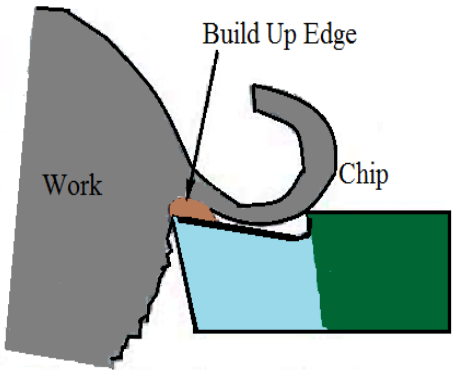

Figure 3.5: Continuous chip with built up edges

3.4 Orthogonal Cutting Model

The first analytical model for cutting force was developed by Merchant [29]. His model was based on the shear plane where the shear force was a maximum and chips were formed by the shearing action. This model had some assumptions, namely cutting was assumed as plain strain or two dimensional. The analysis was made with a large ratio of cutting width to unreformed chip thickness. On the other hand, cutting tool was assumed as a sharp and the chip was considered to be continuous without built up edges. It was also assumed that the shear zone was a thin shear plane.

From the above assumptions the orthogonal cutting force was simplified and described by Figure 3.6. The geometrical relationship between various pairs of force components with cutting geometry is shown in Figure 3.7. It is evident the average sliding velocity along the shear plane V_s, rake face of the tool V_c can be calculated as:

$$\frac{V}{\cos(\varphi-\gamma)} = \frac{V_s}{\cos\gamma} = \frac{V_c}{\cos\varphi} \tag{3.1}$$

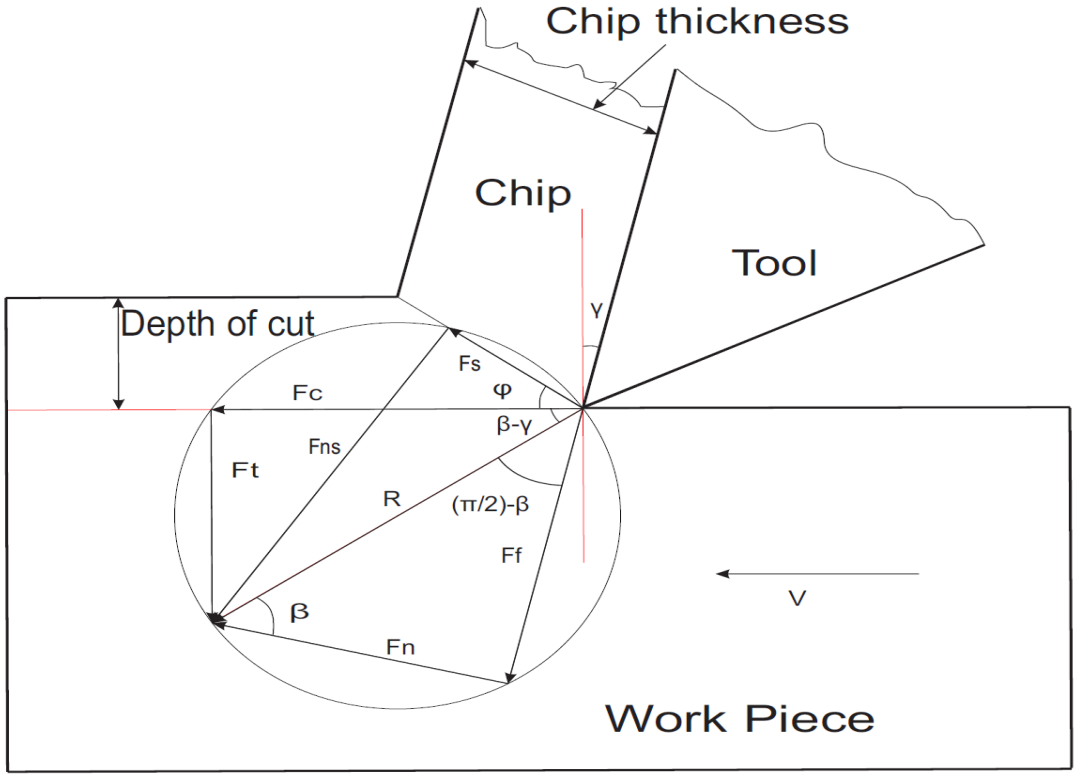

Figure 3.6: Merchant's force circle

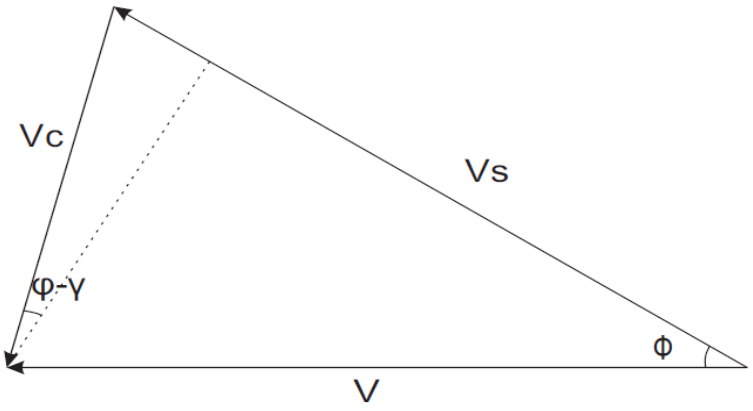

Figure 3.7: Velocity Diagram for orthogonal Cutting

Where, φ and γ are the shear and rake angle, respectively. Again, chip velocity, Vc, can be represented by cutting velocity, V, with chip thickness ratio, r_c, by following equation:

$$r_c = \frac{V}{V_c} \tag{3.2}$$

Then from equation 3.1 and 3.2 the shear angle can be represented by the following equation

$$\tan\phi = \frac{r_c \cos\gamma}{1 - r_c \cos\gamma} \tag{3.3}$$

The force component in the shear plane and the tool faces are related to the cutting forces and thrust force (Figure 3.6).

$$F_s = F_c \cos\varphi - F_T \sin\varphi \tag{3.4}$$

$$F_f = F_c \sin\gamma - F_T \cos\gamma \tag{3.5}$$

$$F_n = F_c \cos\gamma - F_T \sin\gamma \tag{3.6}$$

When the shear angle is predicted and the geometry is fixed, then cutting and thrust force can be calculated from the geometry for certain material with shear flow stress k

$$F_C = \frac{kab\cos(\beta-\gamma)}{\sin\phi\cos(\phi+\beta-\gamma)} \tag{3.7}$$

$$F_T = \frac{kab\sin(\beta-\gamma)}{\sin\phi\cos(\phi+\beta-\gamma)} \tag{3.8}$$

Where, the a,b are the un-deformed chip thickness and width of cut and β is the friction angle. If the friction co-efficient is represented by μ, then

$$\mu = \tan\beta \tag{3.9}$$

Then friction coefficient can be written as

$$\mu = \left(\frac{F_f}{F_n}\right) \quad (3.10)$$

Where, F_f and F_n are the friction force and normal force acting on the rake faces. Again the material flow stress, k has to be determined by suitable material testing methods.

Many other cutting models have been reported, but the Merchant model [29] is one that has the most practice implementations. It provides quantitative value for cutting forces and the dependence of cutting forces with the uncut chip thickness, width of cut, depth of cut, and specific cutting energy. Colwell [40], Shaw et al. [41], Stabler [42] worked on understanding oblique cutting process and reported force model based on the Merchant [29] equation. Though, metal cutting quantities can be determined using the Merchant approach, there are some limitations in estimating several variables in the equations.

During cutting, the material is subjected to large strain and high temperature. This high temperature causes problems in estimating shear flow stress for the machining process using the standard mechanical tests. This can be avoided by using the Johnson-Cook equation [43] as it will be shown latter.

3.5 Shear Angle Models

Several shear angle models have been developed to explain the behaviour of workpiece material during metal cutting process. These models are shown in table 3.1. Analytical approaches to quantify different process parameters were begun during the early 1900s.

Notably, Piispanen [27], Ernst and Merchant [44], and followed by Lee and Shaffer [45] were the pioneers in this field.

Table 3.1: 19th and 20th century internal force angle used in orthogonal cutting [26]

Zvorkin,1890	$\varphi = \frac{\pi}{4} + \frac{\gamma}{2} + \frac{\beta}{2} + \frac{\acute{\beta}}{2}$	Lee and Shaffer,1951	$\varphi = \frac{\pi}{4} + \gamma - \beta$
Ingenious Text,1896	$\varphi = \frac{\pi}{4} - \frac{\gamma}{2} + \frac{\beta}{2}$	Hucks,1951	$\varphi = \frac{\pi}{4} - \frac{\tan^{-1} 2\mu}{2} + \gamma$
Lindner, 1907	$\varphi = \frac{\pi}{4} + \frac{\gamma}{2} + \frac{\beta}{2} + \frac{\acute{\beta}}{2}$	Hucks, 1951	$\varphi = \frac{\cot^{-1} K}{2} - \frac{\tan^{-1} 2\mu}{2} + \gamma$
Ernst and Merchant,1941	$\varphi = \frac{\pi}{4} + \frac{\gamma}{2} - \frac{\beta}{2}$	Shaw, Cook, Finnie,1953	$\varphi = \frac{\pi}{4} + \gamma - \beta + \acute{\eta}$
Merchant ,1945	$\varphi = \frac{\cot^{-1} K}{2} + \frac{\gamma}{2} - \frac{\beta}{2}$	Black and Hung,1951	$\psi = \frac{\pi}{4} - \varphi + \frac{\gamma}{2}$
Stabler,1951	$\varphi = \frac{\pi}{4} + \frac{\gamma}{2} - \beta$	Payton ,2002	$\chi + \beta = \frac{\pi}{4} + \frac{\gamma}{2} = \psi + \varphi$

Early modes are based on the shear plane and continuous chips formation along with two dimensional deformations. Piispanen [27] modeled the shear process of chip formation mechanism as a deck of cards where one card at a time slides forward with cutting tool progresses as shown in Figure 3.8.

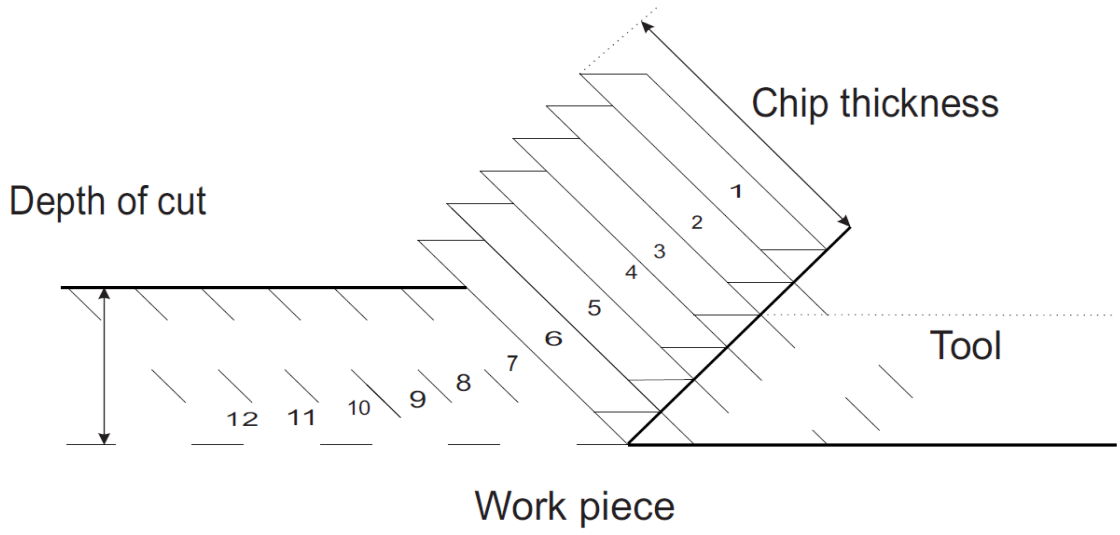

Figure 3.8: "Deck of card" for metal cutting after Piispanen [27]

On the other hand, Ernst and Merchant [44] derived following relation for the shear angle based on the maximum shear stress and minimum total energy:

$$\varphi = \frac{\pi}{4} + \frac{\gamma}{2} - \frac{\beta}{2} \tag{3.11}$$

Merchant then considered the physical properties of the material to improve their model. Merchant assumed that the shear strength of the material as a function of normal compressive stress on the shear plane only. A linear relationship between the shear stress and normal stress on the shear plane was represented by

$$\tau_s = \tau_{so} + K\sigma_s \tag{3.12}$$

Where, τ_{so} is the shear stress of the material under zero compressive stress, K is material constant relating to shear stress and compressive stress and, σ_s is the normal stress in shear plane.

Applying the minimum energy theorem on equation 3.13 Merchant derived a new expression as:

$$\varphi = \frac{\cot^{-1} K}{2} + \frac{\gamma}{2} - \frac{\beta}{2} \tag{3.13}$$

Later, Lee and Shaffer [45] adopted a different approach to develop shear angle relationship. They used slip line field theory. A rigid plastic material behavior was assumed and the internal forces were neglected. The model is applicable to both machining with and without a built up edge. The expression for shear angle reported by them from the slip line field geometry was:

$$\varphi = \frac{\pi}{4} + \gamma - \beta \tag{3.14}$$

Critical re-examining of the previously developed theories of metal cutting was done by Kobayashi and Thomsen [46]. They showed that the modified Merchant theory provides the limiting case of the shear angle for all conditions.

Some other researchers such as Shaw *et al.* [47], Hucks [48] proposed different shear model considering different limitations which can be found in literature [49-50].

3.6 Shear Zone Model

During the early 1960s, Okushima and Hitomi [51] proposed a fan shaped shear zone model for low cutting speed. According to their model, there exists a transitional zone that is bounded by two shear plane. In 1966, Zorev [52] developed his triangular shape shear zone model as in Figure 3.9. He considered shear zone extends below the cutting

tools. The carved boundaries OI and OF are the initial and final boundaries of the shear zone. Material would be sheared along a shear line inside the cutting zone OIF. This is the only model that accounts for the plastic deformation below the cutting edge, even when cutting with sharp tools.

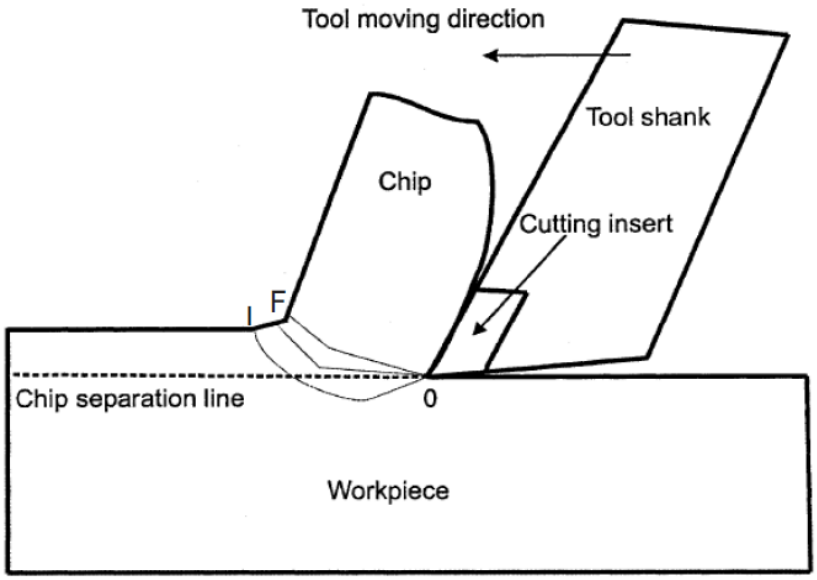

Figure 3.9: Zorev's orthogonal cutting model

Oxley and Welsh [53] expanded the shear zone model. According to them a fan shaped shear zone occurs during low cutting speed and parallel sized zone at high cutting speed rather than single plane. In their study, shearing plane thickness was taken to be one tenth of the shear plane length. A frictional condition was described as shear within a layer of the chip adjacent to the rake face of tool. Again for quantitative prediction, this model takes into account the deformation behavior of work material, strain hardening, influence of high strain rate, and temperature. The expression derived from the model for shear strain was the same as Merchant but derived by a different analytical method. Moreover,

this model eliminates the drawbacks of infinite strain rate across the shear plane. This model was a considerable advancement in field of metal cutting.

3.7 Empirical Models for Cutting

Very few empirical models for metal cutting have been proposed. Most of the empirical models are generally machine and material specific. Those kinds of models are developed to use in industry for different predictions from cutting forces to tool wear. Empirical equations are generally complex relationship between most of the process variables to be fitted from a small number of tests results. The main problems with empirical models are that they lack the description of physical process and have limited ability to generalize the models to different machining conditions and materials. Some of the empirical methods have been described below from an open literature review.

Power law regression methods, relating the turning forces of cutting to the different cutting condition were presented by Waldorf [18]. Again, Zorev [20] developed a force model where he reported that the shear stress be proportional to tensile stress by a set of empirical constants. He also reported that coefficients of friction along the rake face and chip flow direction were both related through an analytical equation with some empirical constants.

There were some other models where key relationship between some important cutting parameters calibrated by experiments can be found in literature [54-55]. Based on the results of a set of orthogonal cutting experiments those models proposed that the shear

stress, shear angle and the coefficient of friction were related to process inputs. Some other models [56-57] reported that the cutting force is proportional to the chip area. The proportionality constants were obtained empirically from different set of experiment data considering basic process inputs like uncut chip thickness and rake angle of tools.

Early studies in machining processes were based on a trial and error approach and empirical understanding. But now research is more on quantitative and qualitative measurements to develop analytical methods to describe process. Some other approaches like finite element methods have been applied to formulate the machining techniques.

3.8 Finite Element Analysis of Machining Process

Metal cutting process is one of the most complex tasks due to large number of constraints affecting the process from different disciplines, such as metallurgy, elasticity, plasticity, heat transfer, vibration, fracture mechanics, contact mechanics, and lubrication [58]. Due to the complexity of the process, numerical approaches have been developed and adopted to replace the direct experimental approach which is time consuming and expensive. Among the numerical techniques, finite element methods are the most common.

With the advancement of the computer technology, finite element methods are successfully used to model and analyze complex problems such as metal cutting , metal forming, contact mechanics, fracture mechanics, etc. With the help of different finite element software the machining process was studied by:

1. Formulating material properties as a function of strain, strain rate, and temperature;
2. Modeling chip tool interface as a function of either sticking or sliding friction.
3. Analyzing the functions, global variables like cutting force, feed force, chip geometry, local stress, strain, and temperature distribution in the work piece can be calculated.

Presently, there are several finite element software packages available, namely ABAQUS, ANASYS, Flex PDE, LUSAS, DYNA-3D (LS-DYNA), and FORGE2. Using these software two types of finite element transit simulations can be performed. They are explicit and implicit. Explicit transit simulations are performed through a large number of small increments which are computationally inexpensive [59]. Computational cost is proportional to the number of elements and inversely proportional to the smallest element size. Generally, implicit simulations are performed through fewer time increments whose size is determined from accuracy and convergence conditions. Again, implicit methods tend to be computationally more expensive since the global set of equations has to be solved with every increment. Computational cost is proportional to the square root of the number of degrees of freedom [60].

Finite element methods involve formulation methods, work piece material constitution, chip separation criterion, and chip tool interface, and mesh considerations. Again there are three kinds of formulation methods for metal cutting process, namely Eulerian, Lagrangian, and arbitrary Lagrangian- Eulerian.

3.9 Different Factors in Metal Cutting

There are different factors that directly affect machining such as friction, ploughing, wear etc. Among them the effect of friction and ploughing are described below because of their close relation with present research.

3.9.1 Friction in Metal Cutting

Friction plays a very important role in chip formation. Friction occurs in two regions during metal cutting, at the tool – chip interface and at the tool work piece interface.

Earlier studies of orthogonal machining have considered friction at the rake face similar to those of ordinary sliding forces. Merchant [29] assumed that the friction on rake face follow well known Amonton's Law of Sliding. Later Amonton's law of friction was verified by Coulomb. Others such as Bowden and Tabor [61] described friction in nachining based on adhesion theory of friction. Usui and Takayama [62] studied stress distribution in chip- tool interface using photoelastic tools. Results indicated that the shear stress remained constant for half of the tool chip contact length from the tool tip. Eventually, it decreased to zero in the second half. On the other hand, normal stresses were increasing towards the cutting edges. The region close to the tool cutting edge where an only normal stress varied was called the "Sticking zone" and the layer of materials close to rake face of the tool were assumed to be sticking to the tool. The zone where both normal and the shear stress varied was known as the "Sliding zone" [62].

3.9.2 Ploughing in Metal Cutting

Generally the tool edge cannot be perfectly sharp. The contribution of edge ploughing to cutting forces is typically neglected in most of the force model and thought to be less than 5% of the total force [63]. The ploughing mechanism has been studied for more than 40 years in attempts to explain various cutting phenomena.

Waldorf [63] calculated the ploughing force based on slip line field theory. A slip-line field considers the deformation below a rounded cutting edge in orthogonal machining. The model was based on a dead-metal zone formed at the rounded edge, a raised prow of material ahead of cutting, and a wedge of deformation below the dead-metal zone dependent on frictional stresses there.

A basic slip-line field is shown in the Figure 3.10. This can be simplified by assuming a negligible prow (ρ=0) and a friction stress on the dead-metal zone equal to the machining shear stress of the work material .Since the angle that slip-lines meet the dead-metal zone depends on this friction condition, the latter simplification implies that η=0 (Figure3.10 region III) and the slip-line "field" collapses to a single slip line (i.e., δ=0 Figure3.10 region II). The cutting and thrust forces on the lower boundary of the dead-metal zone due to ploughing can then be written as:

$$F_{CP} = klr_e \tan\left(\frac{\pi}{4} + \frac{\gamma}{2}\right) \quad (3.15)$$

$$F_{TP} = klr_e \left[1 + \frac{\pi}{2}\right] \tan\left(\frac{\pi}{4} + \frac{\gamma}{2}\right) \quad (3.16)$$

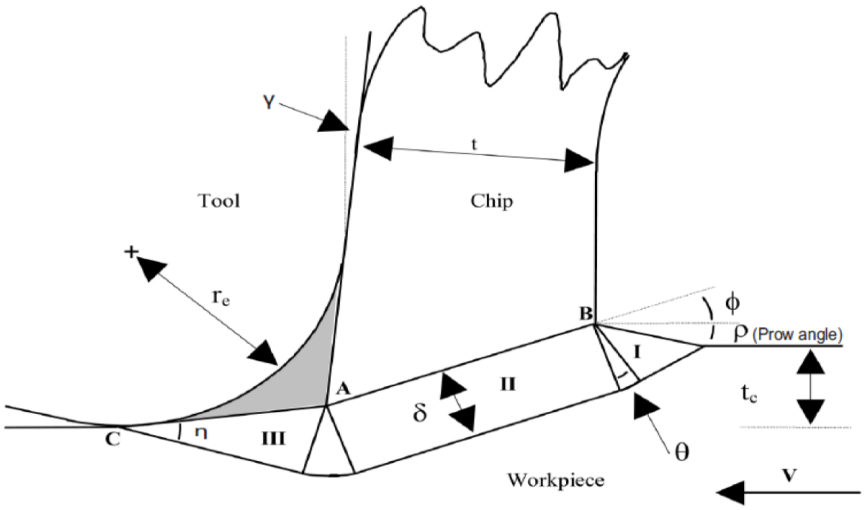

Figure 3.10: *Slip-Line field for Ploughing [63]*

Where, the cutting width l can be expressed in terms of the approaching angle θ_a and the nose radius, r_n, as given by Equation 3.17:

$$l = r_n \left[\theta_a + \sin^{-1}\left(\frac{b}{r_n}\right)\right] + \frac{a - r_n(1-\cos\theta_a)}{\sin\theta_a} \qquad (3.17)$$

3.10 Machinability of Metal Matrix Composites

The term "Machinability" has treditionally referred to the ease with which a material can be machined with acceptable quality under given set of conditions. But machinability is a difficult term to define and quantify because large number of variables are involved in it. Cutting forces, power consumed, tool life, and surface finish are only some of the factors to be considered when referring to machinability. The difficulty arises because of the dependence of these factors on a large number of variables such as work material, tool

geometry, cutting conditions, machine tool rigidity. Materials with good machinability require less power to cut but materials with lower machinability require special arrangements for machining. So, the machinablity of materials has significant economic impact. On other hand, properties like hardness and stiffness which make metal matrix composites appealing to industry but can present major challenges when machining. Wide spread application of MMCs will not possible without the solution for the shortened tool life and material sub surface damages encountered during cutting operation. So to minimize the processing cost, it is important to understand the mechanics of machining MMC.

In this section the attention will be focused on the cutting forces, surface integrity and wear. It is interesting to note that most of the studies carried out on machining are based on experimental results and very few are of them are analytical.

3.10.1 Cutting Forces

Prediction of cutting forces is necessary to estimate power requirement of a machine tool and to estimate the force on tool components such as bearings, jigs, and fixtures. Very little research has been done to predict the cutting force involved in MMC machining.

Hoecheng *et al.* [64] first studied the effect of speed, depth of cut, rake angle, and cutting fluid during machining MMCs. He reported that the increase in reinforcement percentage causes an increase in cutting force and decrease in negative rake angle causes a decrease

in cutting force and tool life. Most of the early studies were either on experimental studies that compare different tools or empirical and numerical studies related to tool life.

First real analytical force model was developed by Kannan *et al.* [65]. They estimated the cutting force based on the energy consumed in the primary, secondary shear zone, and reinforcement particle displacement and fracture. According to the model, energy per unit volume is

$$e = E_p + E_s + E_d \tag{3.18}$$

Cutting force was calculated by multiplying the width of cut and under deformed chip thickness. Here the energy consumed in the secondary deformation zone was assumed as one third of that in the primary shear zone. Although this assumption is true for monometallic material, it is questionable for the case MMCs. Again only the force in the cutting direction was calculated from the total energy consumed during machining. In addition, energy due to ploughing was not considered.

Pramanik *et al.* [4] developed an analytical model to predict the cutting force and the thrust force. In this model, the total force was considered as the sum of chip formulation force, ploughing force, and particle fracture force. The chip formation force was obtained by using Merchant [29] analysis but those due to matrix ploughing deformation and particle fracture were formulated respectively with the aid of the slip-line field theory of plasticity and the Griffith theory of fracture. However, the chip-tool friction force due to reinforcement particles was not considered.

Recently, Dabade *et al.* [66] considered chip-tool interface friction to predict cutting forces in oblique cutting. They provided an analytical model to compute the machining force components in three directions during oblique cutting. Unfortunately, the authors did not consider the effect of particle debonding and ploughing force.

3.10.2 Tool Wear and Tool Life

Tool wear is a crucial factor of machinablity for any materials. The tool wear includes several modes of wear like flank wear, crater wear etc. Flank wear is the most dominant mode of wear which influences the tool life, when cutting MMCs.

Hard abrasive reinforcement particles in MMCs provide a constant threat to the cutting tools and forming die. Though new production techniques provide new processes to produce net shape components to minimize machining, final machining and finishing are still required to obtain suitable dimension and quality. Efficient and economic machining of these materials is required for proper dimension and surface finish.

The machinability of metal matrix composites is comparatively poor because the tool wear rate is high and quality of surface finish is on the lower side. Improper tooling and machining conditions also often lead to tool-wear and subsurface damage [67]. Most of the early research has covered the effect of machine parameters and properties of MMCs on mechanism of tool wear.

Tomac and Tonnessen [68] investigated the effect of cutting conditions on the various aspects of machinability (e.g. tool wear, cutting forces, and surface finish) during machining Al-SiC MMCs with PCD and coated tungsten carbide tools. They developed a tool life relationship for cutting speed, lower than 100 m/min. They reported that PCD tools had over 30 times longer tool life than carbides under similar cutting conditions. According to them primary wear mechanism being abrasion of the SiC particles. Similar results were reported by several other researchers [69-71].

Lin *et al.* [72] studied MMCs and the dependence of tool wear on the percentage of reinforcement in the MMCs. They observed that the abrasive tool wear was accelerated when the percentage of the reinforcement in the MMC exceeded a critical value. In their machining tests measured tool wear was found to be increasing and constant surface finish with the increasing speeds (At high speeds 300-700m/min).

The effect of different cutting conditions and tools on the machinability of MMCs has been studied by different researchers. Most of the publish literature indicate that only Diamond tools (PCD and Chemical Vapor Deposition) provide useful tool lives. Diamond tools have higher hardness than the reinforcements and do not have chemical affinity to react with the work material [73]. On the other hand diamond tools are expensive in comparison to the other tools. Hence, ceramic tools and cemented carbide tools were studied by different researchers. They found that ceramic tools are unsatisfactory and the cemented carbide tools are good at low cutting speed and higher feed rates. Few researches also reported the effect of coating on the tool wear for

different kinds of tools. Andrews *et al.* [74] compared the performance of PCD and carbide tools with diamond coating by Chemical Vapor Deposition (CVD) and observed that PCD inserts perform much better than CVD diamond coated tools.

Several researchers reported abrasion wear appears to be the predominant wear mechanism [70-71]. El Gallab and Sklad [75] studied the performance of PCD tools and concluded that the main wear mechanisms with these tools were abrasion and micro-cutting of tool material manifested in the form of grooves on the tool face parallel to the chip flow direction. The grooves on the rake face were filled with smeared work materials and form a built-up edge, which seemed to be beneficial since it protected the tool rake from further abrasion. However, for all the tested tools the tool life was limited by excessive flank wear due to abrasion. Flank wear is a result of intensive rubbing between the newly generated work surface and the flank face in the vicinity of the cutting edge. The authors also noted that the cutting parameters play a determinant role in the tool flank wear. Tool wear may be minimized by increasing feed rate and cutting speed. Higher cutting speeds are associated with an increase of the cutting temperatures which led to the formation of a protective built-up layer [75]. Barnes *et al.* [76] have reported on the effect on hot machining of MMCs. They carried out machining at 200-400°C. For low cutting speeds and preheated MMC they reported increased tool life due to Built -Up -Edges. Pramanik *et al.* [77] and several other researchers used finite element modeling to investigate the tool - particle interaction during machining of MMCs.

From the literature review on the wear mechanism of MMC, it can be concludes that-

1. PCD are the preferred tools in machining MMCs due to their hardness, high thermal conductivity, low coefficient of friction and inert nature. Among the PCD tools, course grained PCD inserts were found to be most suitable.
2. Lower cutting speeds escalate the formation of BUE in front of tool tips. This controlled BUE generally helps to improve tool life and reduce tool wear.
3. Higher feed rates also increase the tool life and decrease the tool wear. This happens because higher feed rate tend to soften the metal matrix
4. Abrasion by the reinforcements is the main cause of wear in both primary and secondary flank surfaces.
5. Some attempts have been made to examine wear and tool life with finite element analysis and hot machining.

3.10.3 Surface Quality and Integrity

MMCs are a combination of soft matrix with hard reinforcement particles or fibers. Chips are formed by either shearing of the matrix or pulling or fracture of the hard reinforcement particles. Due to fracture and crack formation in the matrix, material surface and subsurface damage are expected in the workpiece. A review of literature shows that the surface and subsurface damage occurs in MMCs for both conventional and unconventional machining. Some [78-80] suggest that the grinding and abrasive blasting can be utilized to increase surface integrity.

Ceramic particle cracking and fracture generally affect the surface integrity [80]. The particles pulled out of the matrix by the tools during cutting operation leaves some voids, holes, and craters that can act as a source of fatigue cracks. Severe damage to the machined surface can be caused due to the high temperature gradient developed during plastic deformation of chip forming process. These impose residual stresses along the micro and macro cracks on the matrix.

The matrix is subjected to high compressive stress by the cutting tool and this can result in non homogeneous plastic deformation. Subsequently, small pieces of the work piece material ad hear to the cutting tool and weld to it firmly due to high temperature and pressure during cutting. As the cutting progresses, the conglomeration of the work piece material on the cutting tool edge becomes larger and thus gets unstable. Consequently, when a chip shears off, it eventually creates micro-defects on the produced surface. Again, high temperatures are reached due to deformation and friction between the tool flank and the work piece. Rapid cooling upon removal of cutting load induces thermal stresses in the material. Hence there will be work hardening and residual stress in the machined surface layer. Several authors tried to measure the residual stress induced in the matrix and reinforcements [80]. In the work of Lee *et al.* [81] the depth profiles of residual stresses in the both Al matrix and SiC reinforcements were obtained. From their work it can be concluded that the annealing introduced hydrostatic tension in Al matrix and hydrostatic compression in the SiC particles.

Cutting geometry has also effect on the surface finish during machining of MMCs. According to Lane *et al.* [82] the best surface finish obtained with slightly worn cutting tools is due to the stabilization of nose radius and cutting edge radius. Dabade *et al.* [66] used wiper in cutting edge geometry, which performs burnishing operation by the extended cutting edge. He reported better surface finish with wiper insert. El-Gallab and Sklad [75] reported that the negative rake angles caused greater surface roughness due to clogging of chips between the tool and machined surface.

In machining MMCs, cutting parameters are also significant factors which influence the surface quality. Paoletti *et al.* [83] observed through experiment that the surface roughness was reduced with the increase in feed rate due to reduction of flank wear. They also reported that surface finish improved with the increase of cutting speed at same feed rate. It was also found that hardening increases with the increase of any cutting parameters.

3.10.4 Effect of Coolant Application

Different studies were carried out in the past to understand the effect of cutting fluid on the machinablity of MMCs [84-85].The findings are somewhat contradictory with each other. Hung *et al.* [86] reported that the application of cutting coolant did not have any influence on the tool life, surface finish, or cutting force when machining with new tools and different cutting speeds. Cronjager *et al.* [87] studied drilling MMCs with different particular reinforcements, and reported that tool life decreased to one sixth due to use of

coolant. They proposed that the reason was that the coolant decreased the temperature in the chip formation zone which helped to matrix to retain its strength, which leads to high tool wear. Barnes *et al*. [88] also found similar results like. On the other hand, Shetty *et al.* [89] worked with water steam as a coolant and reported that the use of coolant reduced the cutting force and temperature but increased tool wear. These findings were contradictory to previous findings. Thus, the effect of coolant application is an area needing further study.

3.11 Summary

The analytical approaches to understand the mechanics of machining processes have been tackled by many researchers. Usually, all the methods are based on two main principals either single shear plane or shear zone. Most of the approaches oversimplify the cutting condition and deformation zone. However, adequate material properties are usually not available since material tests are performed under different conditions. On the other hand, the conventional machining of MMC leads to tool wear and subsurface damage due to abrasive nature of the reinforcement. These ultimately increase the machining time and all related cost. The main objective of this thesis is to develop an analytical force model to predict cutting forces during the machining MMCs. Proper understanding of tool wear and the characteristic and deformation behavior of MMC are essential to develop a proper model to predict cutting forces.

CHAPTER 4

A Force Model for Machining MMC

4.1 Introduction

In this chapter, a thermo-energy based analytical model for predicting cutting forces during machining Metal matrix composites (MMC) is presented. Several aspects of cutting mechanics were considered to estimate the generated forces including shearing force, ploughing force, and particle fracture force. Shearing force, ploughing force, and particle fracture force calculations are described in section 4.2.

4.2 Developing the Thermo-Analytical Force Model

MMCs are the combination of abrasive particle reinforcement and the ductile alloys. Due to their specific nature, the resultant forces generated during machining MMCs are mainly caused by:

a) Shearing of the matrix metal to form a chip;

b) Ploughing due to squeezing of metal under rounded part of the tool edge;

c) Particle fracture or pullout from the MMC matrix.

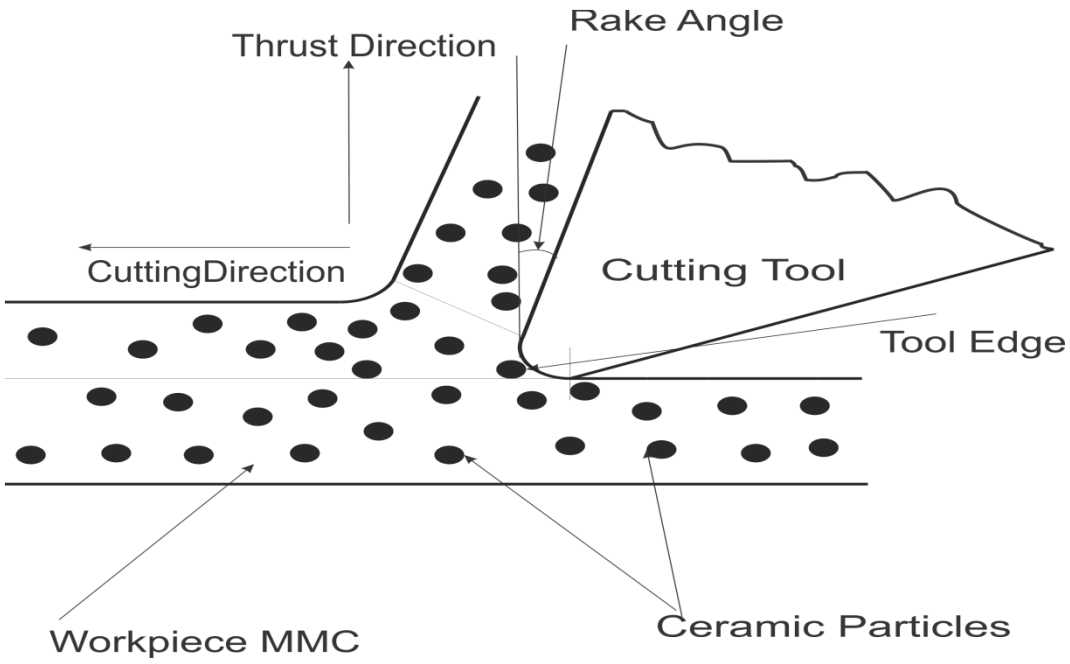

Figure 4.1: Schematic diagram of the machining process for MMC

Therefore, the resultant cutting force F_C and thrust force F_T can be written in the form of Equation (4.1) and Equation (4.2), respectively.

$$F_C = F_{CC} + F_{CP} + F_{CD} \tag{4.1}$$

$$F_T = F_{TC} + F_{TP} + F_{TD} \tag{4.2}$$

Where, F_{CC} and F_{TC} are the forces by the cutting ductile matrix; F_{CP} and F_{TP} are ploughing forces; F_{CD} and F_{TD} are the forces caused by the debonding and fracture of reinforcing particles.

4.2.1 Chip Formation Force Due to Shearing (F_C)

At higher cutting speeds, the thickness of the shear zone is reduced to a thin shear plane [90, 91]. Due to the simplicity of the shear plane models and relatively high cutting speeds normally used during machining MMCs with ceramic tools, Merchant's analysis is selected in this study to determine the chip formation force. Accordingly, forces in cutting and thrust directions can be determined from Equation (4.3) and Equation (4.4).

$$F_{CC} = \frac{kab\cos(\beta-\gamma)}{\sin\phi\cos(\phi+\beta-\gamma)} \tag{4.3}$$

$$F_{TC} = \frac{kab\sin(\beta-\gamma)}{\sin\phi\cos(\phi+\beta-\gamma)} \tag{4.4}$$

Where a and b are equivalent depth of cut and feed which are determined using equivalent cutting edge concept. The shear strength of the matrix is represented by k which is a constant that can be determined by various equations. However, during machining of MMCs, high strain rate and temperature is observed. Therefore, a material constitutive equation that accounts for temperature and strain rate vary, has to be considered. The material flow stress k in equation 4.3 and 4.4 can now be represented by the following Johnson-Cook constitutive equation.

$$k = 1/\sqrt{3}[A + B\varepsilon^n][1 + C\ln\dot{\varepsilon}]\left[1 - \left(\frac{T-T_r}{T_m-T_r}\right)^m\right] \tag{4.5}$$

Where, A, B, C, and m are the Johnson-Cook constant which are determined by suitable material testing methods. The equivalent shear strain rate is represented by $\dot{\varepsilon}$, the

equivalent shear strain by ε. The material temperature, melting point temperature and room temperature are represented by T, T_m, and T_r respectively.

The equivalent shear strain, shear strain rate and the temperature in the primary shear zone are given in Table 4.1. Where, C_0, K_s, W, h are represented by Kronenberg constant, unit force, thermal conductivity, and specific heat of material, respectively.

Table 4.1 Processing parameters for the primary shear zone

Parameters	Equations	References
Equivalent shear strain(ε)	$\varepsilon = \frac{1}{2\sqrt{3}} \frac{\mathrm{Cos}\,\gamma}{\mathrm{Sin}\varphi\,\mathrm{Cos}(\varphi - \gamma)}$	[92]
Temperature (T)	$T = \frac{C_0 K_s V^{0.44} A_c^{0.22}}{W^{0.44} h^{0.56}}$	[93]
Equivalent shear strain rate (ε̇)	$\dot{\varepsilon} = \frac{2.59\, V\varepsilon \sin\varphi}{a}$	[92]

The shear angle ϕ can be determined from the measured chip thickness. The friction angle β was calculated considering the two body and three body friction on the chip-tool interface, as shown in Equation (4.6).

$$\beta = \tan^{-1}\left(\frac{F_P + F_r}{F_N}\right) \quad (4.6)$$

Where, F_p and F_r represent two body rolling abrasion and three body rolling friction. F_N represents normal frictional force.

4.2.1.1 Determination of Equivalent Cutting Edge (θ_{ae})

Since the tools have a nose radius, their influence was taken into account using the concept of equivalent cutting edge. The straight and round parts of the cutting edge are replaced by a single straight cutting edge which was taken as the line joining the extreme points of the engaged cutting edge as suggested by Colwell [94]. The equivalent cutting edge θ_{ae} can be represented by following equation.

$$\theta_{ae} = \cot^{-1}\left(\frac{r_n + f/2}{d}\right) \text{ where }, d > r_n \quad (4.7)$$

$$\theta_{ae} = \cot^{-1}\left(\frac{(2r_n - d^2)^{1/2} + f/2}{d}\right) \text{ where}, d < r_n \quad (4.8)$$

Where, d is depth of cut, f is feed rate and r_n is nose radius.

Now using equivalent cutting edge, a and b are determined using equation (4.9) and (4.10)

$$a = \frac{d}{\sin\theta_{ae}} \quad (4.9)$$

$$b = f\sin\theta_{ae} \quad (4.10)$$

4.2.1.2 Determination of Friction Angle (β)

When the chip slides along the cutting tool rake face, energy has to be supplied to overcome the friction in this zone. For MMCs, it has been realized [95-96] that the chip-tool friction is mainly characterized by the two body rolling abrasion (F_p) and the three body rolling friction (F_r) as shown in Equation (4.11) (Figure 4.2 and 4.3).

$$F_f = F_p + F_r \quad (4.11)$$

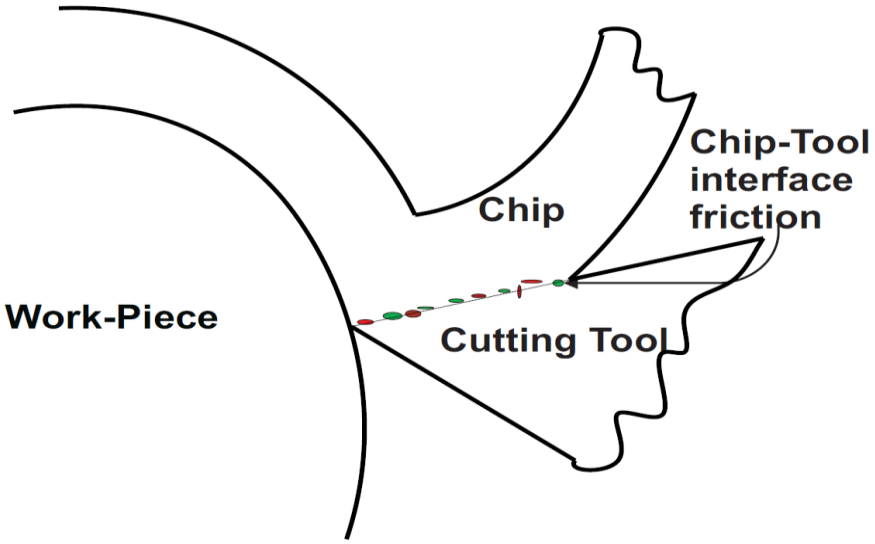

Figure 4.2: Contact between abrasive particle and rake face of tool

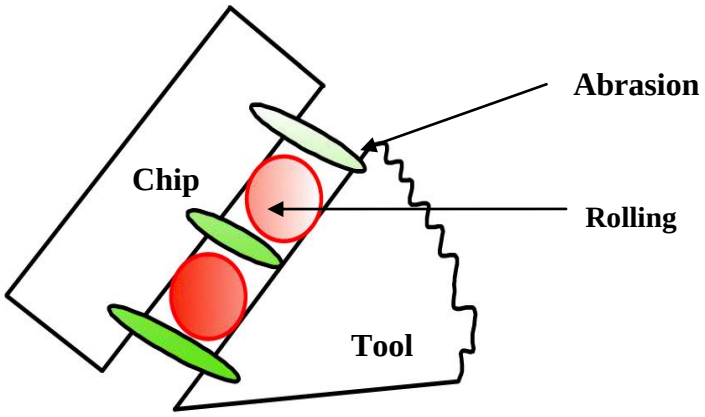

Figure 4.3: The two body rolling abrasion and the three body rolling friction

In the two-body abrasive wear studies by Jiaren *et al.* [97], the shape of reinforcement particles was assumed to be spherical, as shown in Figure 4.4.

Based on this contact geometry, the two body rolling abrasion in chip-tool interface can be calculated by the following equation.

$$F_p = N_p A_i 3\sigma_{y(tool)} q \quad (4.12)$$

Where

$\sigma_{y(tool)}$ is yield strength of tool material.

q is the fraction of the particle involved in two body abrasion (taken as 45%) [65].

The number of abrasive particles involved in the tool-chip friction N_p is

$$N_p = \frac{V_p b a}{\pi R^2} \quad (4.13)$$

In which, V_p is the volume fraction of reinforcement.

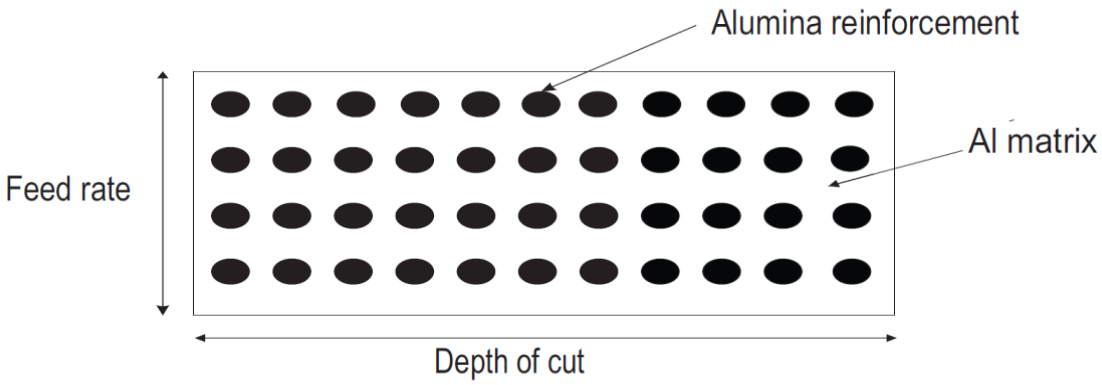

Figure 4.4 : Enlarged view (cross-section of chip tool interface contact)

The contact area A_i (Figure 4.5) and apex angle (θ_p) can be calculated from Equation (4.14) and Equation (4.15) respectively.

$$A_i = \frac{R^2}{2}\left(\frac{\pi}{180}(2\theta_p) - \sin(2\theta_p)\right) \quad (4.14)$$

$$\mathrm{Cos}(\theta_p) = 1 - \frac{\delta_{Po}}{R} \quad (4.15)$$

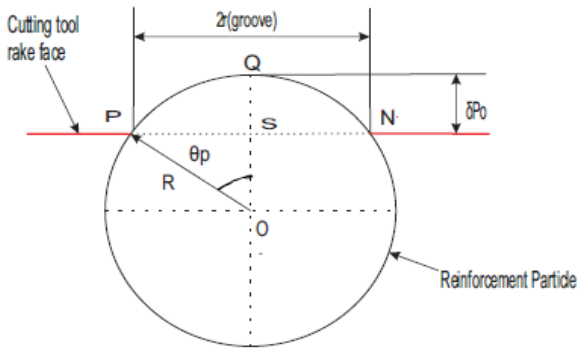

Figure 4.5: Contact between abrasive particle and rake face of tool [66]

Frictional force due to three-body rolling F_R can be obtained from

$$F_R = \mu_{three-body} F_N \tag{4.16}$$

Friction coefficient for the three bodies rolling is give by equation (4.17) based on the studies on ploughing forces, friction coefficient and effect of grit size on abrasive wear as given in Venkatachalam and Liang [98], and the model of Sin *et al.* [99] model .

$$\mu_{three-body} = \frac{k_{(tool)}}{\pi H_t}\left(\frac{2R}{r_{groove}}\right)^2 \left\{1 - \left[1 - (\frac{r_{groove}}{2R})^2\right]\right\}^{1/2} \tag{4.17}$$

$$\text{Where, } r_{groove} = \sqrt{R^2 - (R - \delta_{Po})^2} \text{ (From Fig 4.5)} \tag{4.18}$$

$$k_{(tool)} = \text{shear stress of tool material} = \frac{\sigma_{y(tool)}}{2} = \frac{H_t}{6} \tag{4.19}$$

Normal load is applied on the fraction of particles on the chip across the tool contact surface. Total normal forces at chip-tool interface (F_N) can be calculated from following equation.

$$F_N = F_{N1} \times N_p \times q \tag{4.20}$$

Where, F_{N1} is the normal force on individual abrasive particle. In present model refer to figure 4.5 where full plastic deformation of the tool occurs and due to abrasive sliding against tool face. Therefore, normal force acting on the single abrasive particle is obtained from the analogy of abrasive wear on multiple contact condition mentioned in Ref. [97] and given by

$$F_{N1} = 2.9\pi R\sigma_{y(tool)}\,\partial_{Po} \tag{4.21}$$

Where, ∂_{Po} is critical value of relative penetration which is calculated by following equation.

$$\partial_{Po} = \left(\frac{9\pi}{4}\right)^2 \left(\frac{\sigma_{y(tool)}}{\dot{Y}}\right)^2 R \tag{4.22}$$

Where $\dot{Y}$ can be calculated for chip-tool interface considering young modules of the tool and the MMC

$$\frac{1}{\dot{Y}} = \frac{(1-\upsilon_1)^2}{Y_1} + \frac{(1-\upsilon_2)^2}{Y_2} \tag{4.23}$$

Where, Y_1,Y_2 and υ_1, υ_2 are the elastic modulus and poison ratio for work piece and tool materials.

4.2.2 Ploughing Force

Based on slip line field model representing the deformation below a rounded cutting edge in orthogonal machining, the ploughing force components can be calculated by considering the edge radius r_e [63].

$$F_{CP} = klr_e \tan\left(\frac{\pi}{4} + \frac{\gamma}{2}\right) \tag{4.24}$$

$$F_{TP} = klr_e \left[1 + \frac{\pi}{2}\right] \tan\left(\frac{\pi}{4} + \frac{\gamma}{2}\right) \quad (4.25)$$

Where, the cutting width l can be expressed in terms of the approaching angle θ_a and the nose radius r_n, as shown in Equation (4.26).

$$l = r_n \left[\theta_a + \sin^{-1}\left(\frac{b}{r_n}\right)\right] + \frac{a - r_n(1 - \cos\theta_a)}{\sin\theta_a} \quad (4.26)$$

4.2.3 Particle Fracture and Debonding Force

While the tool moves in the cutting direction, the hard abrasive reinforcement particles in the ploughing zone are fractured. In this model, the fracture force is calculated based on the fracture energy. If the fracture energy per particle is denoted by U, the fracture force in the cutting and thrust directions can be calculated by Equation (4.27) and Equation (4.28).

$$F_{CD} = UabN_p \times q \quad (4.27)$$

$$F_{TD} = F_{cp} \times \tan\delta \quad (4.28)$$

Where δ is the angle between the resultant force and cutting direction which can be found from the following equation.

$$\sin\delta = \frac{r_e(1 + \sin\gamma)}{2R + 2r_e} \quad (4.29)$$

In the current study, the cracking damage of the ceramic particle is assumed to be controlled by the stress on the particle and the statistical behavior of strength of the

particle. Therefore, the change in potential energy of the composite due to debonding damage is a function of volume fraction of the reinforcement and material properties, as shown in Equation (4.30).

$$\frac{dU}{d\lambda} = \left(\frac{(1-\upsilon)^2}{Y}\right)\pi\sigma^2\lambda w \tag{4.30}$$

Where λ is the initial interface crack length, w is initial interface crack width which are assumed to be $1\mu m$.

Fracture Stress σ for the ceramic particle can be found from Griffith formula.

$$\sigma = \frac{K_c}{\sqrt{2R}} \tag{4.31}$$

By integrating the equation (4.30) from initial crack length to the circumference of the particle, the strain energy consumed for debonding process for a particle can be determined by following equation.

$$dU = \int_{1\mu m}^{2\pi R}\left(\frac{(1-\upsilon)^2}{Y}\right)\pi\sigma^2\lambda w\, d\lambda \tag{4.32}$$

4.3 Calculation of Predicted Cutting Forces

Using the information presented in previous section, prediction of the cutting force according to the presented model is done through three steps. They are:

1. Calculation of the chip formation force (Figure 4.6) ;
2. Calculation of the ploughing force;
3. Calculation of the debonding force (Figure 4.7).

Friction force for the calculation of chip formation force has been calculated through the steps shown in Figure 4.8. The three diagrams illustrate the way the equations were used in the calculation process.

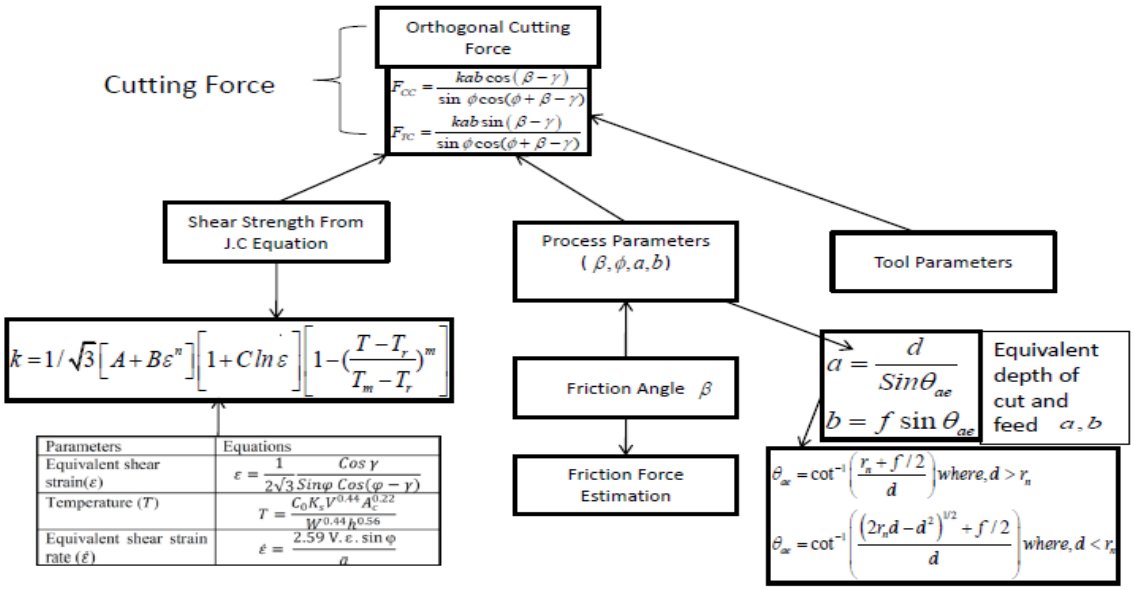

Figure 4.6: Calculation of chip formation force

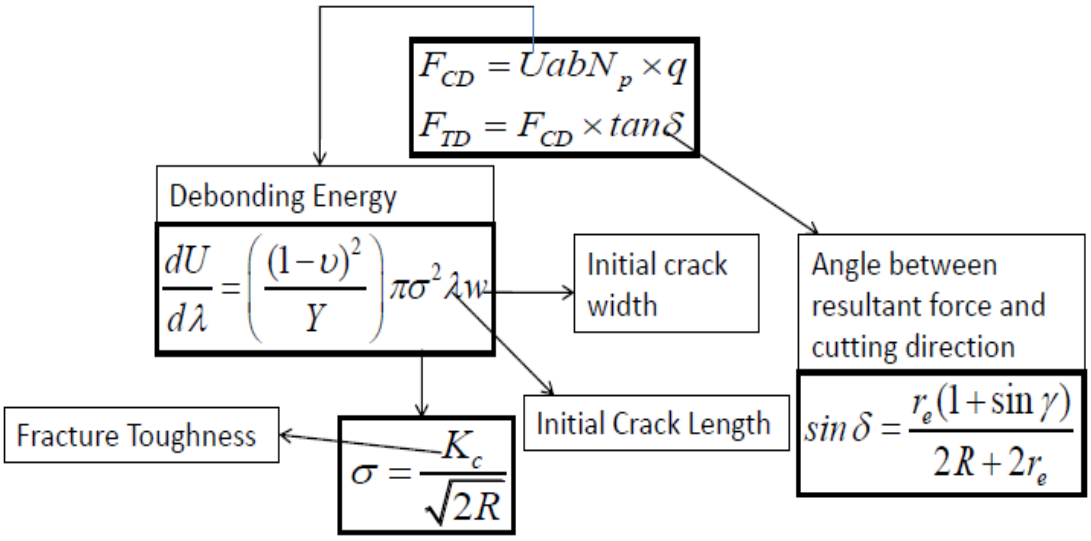

Figure 4.7: Calculation of debonding force

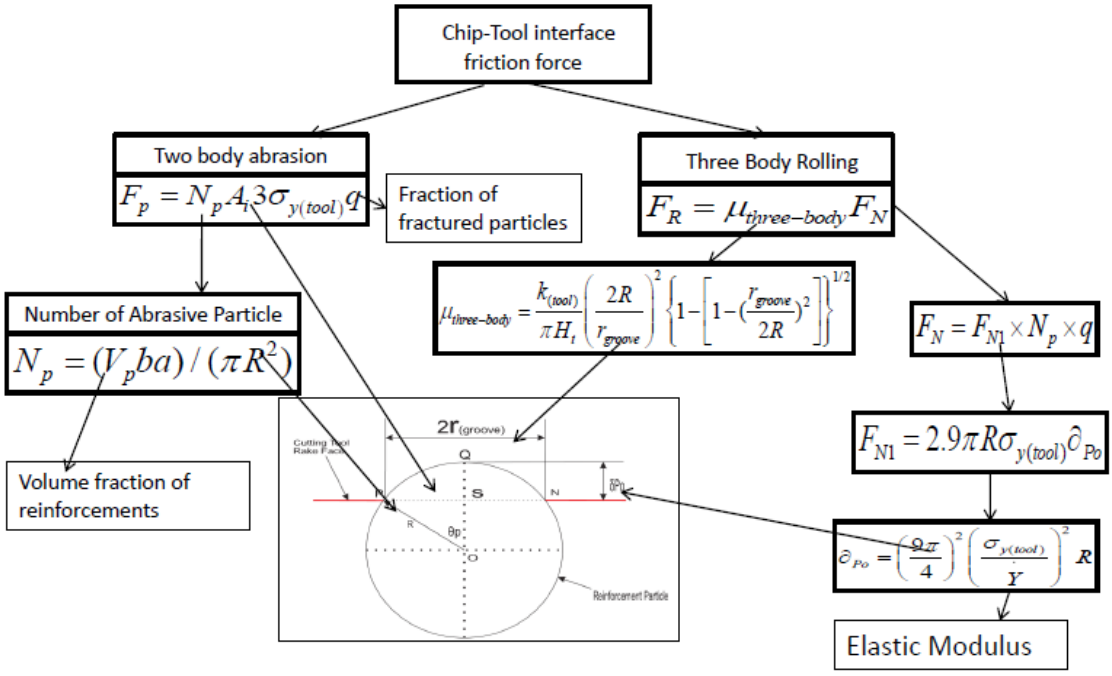

Figure 4.8: Calculation of friction force

4.4 Summary

In this chapter, the "Thermo Mechanical Analytical Model" has been developed for predicting the forces when machining MMCs. The generated forces have been estimated from several aspects of cutting mechanics such as: shearing force, ploughing force and particle rolling fracture force. Present model is based on Merchant's analysis, J-C equation, slip line field theory and Griffith theory. Moreover it can predict frictional force in chip-tool interface and forces due to ploughing.

CHAPTER 5

MODEL VERIFICATION

5.1 Overview

In this chapter, verification of the proposed model is presented. In order to verify the developed model, cutting test data was obtained from the experiments of Kannan [17]. A synopsis of the experimental procedure and the results are presented in section 5.2 and 5.3, respectively. In section 5.4 the model validations are presented by comparing predicted cutting force with measured force. A summary of findings has been presented in section 5.5.

5.2 Experimental Procedure

5.2.1 Cutting Tool and Work Materials

Kannan [17] carried out experiments on two types of aluminum MMCs reinforced with Al_2O_3 particles:

a) Al7075 MMC reinforced with 10% and 15% volume fraction of Al_2O_3, with an average particle size of 15 μm and 17 μm respectively;
b) Al6061 MMC reinforced with 10% and 20% Al_2O_3, with an average particle size of 17 μm and 23 μm respectively;

The cutting tool used was the ceramic tool with 6° rake angle and 86° approach angle. The nose radius and the edge radius were 0.4mm and 5μm respectively.

Cutting tests were conducted at different feeds (0.lmm, 0.15mm, 0.175mm, and 0.2mm) and at constant cutting speed (60m/min) and depth of cut (3mm). The tests were conducted in such a manner that the volume of metal removed for a particular cutting condition for all the materials was kept constant. Cutting forces were measured with a Kistler three-component piezoelectric dynamometer (Kistler™ type 9251A). The variation in the cutting forces was checked by repeating the cutting tests on the same work piece materials. The effect of reclamping the work-piece on the forces generated was also investigated. After each test, the chip thickness was measured so that the shear angle can be determined by following Equation 5.1

$$\tan\phi = \frac{r_c \cos\gamma}{1 - r_c \cos\gamma} \tag{5.1}$$

Where, r_c is chip thickness ratio. Measured chip thickness ratios from the experiment are shown in Figure 5.1 for different MMCs.

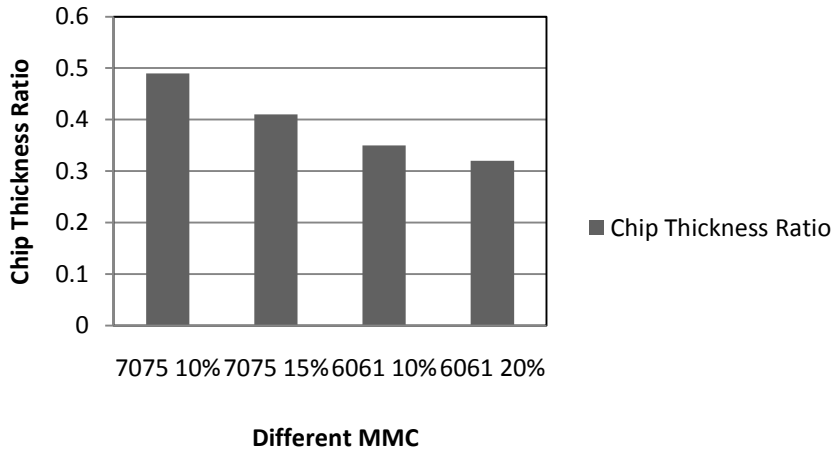

Figure 5.1:Chip Thickness ratio for different materials [17]

5.3 Characteristics of Measured Cutting Forces

Figures 5.2 and 5.3 show the variation in force components during machining 7075 MMC with 10% and 15% Alumina reinforcements under various feed rates. Figures 5.4 and 5.5 show the force components for machining 6061 MMC with 10 and 20% alumina reinforcements. The results are the average of the three cutting tests. An increase in feed rate resulted in a corresponding increase in cutting and thrust force components for all the cases considered.

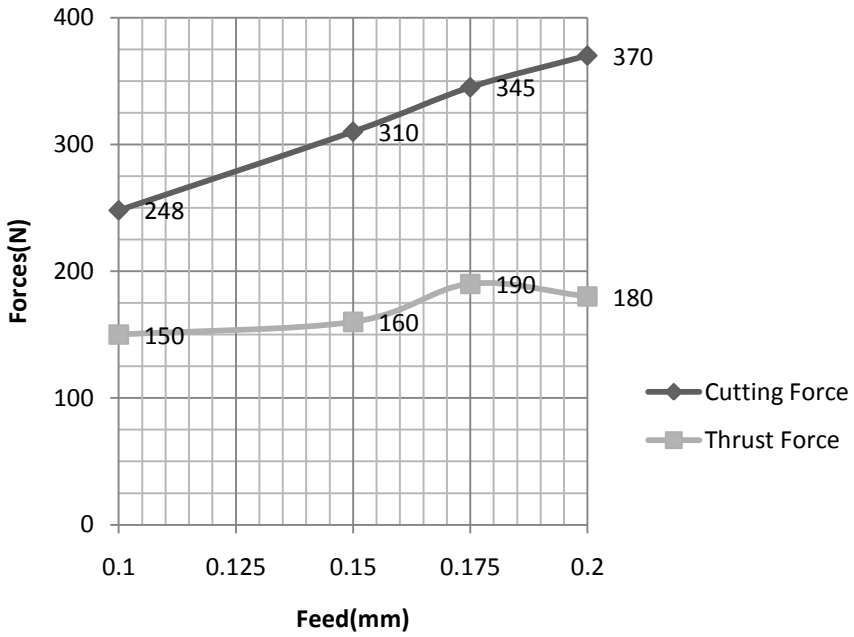

Figure 5.2: Measured forces Al 7075 10% Alumina

(Vc =60m/min;d=3m; r_n=0 .4mm; r_e=5μ m [17]

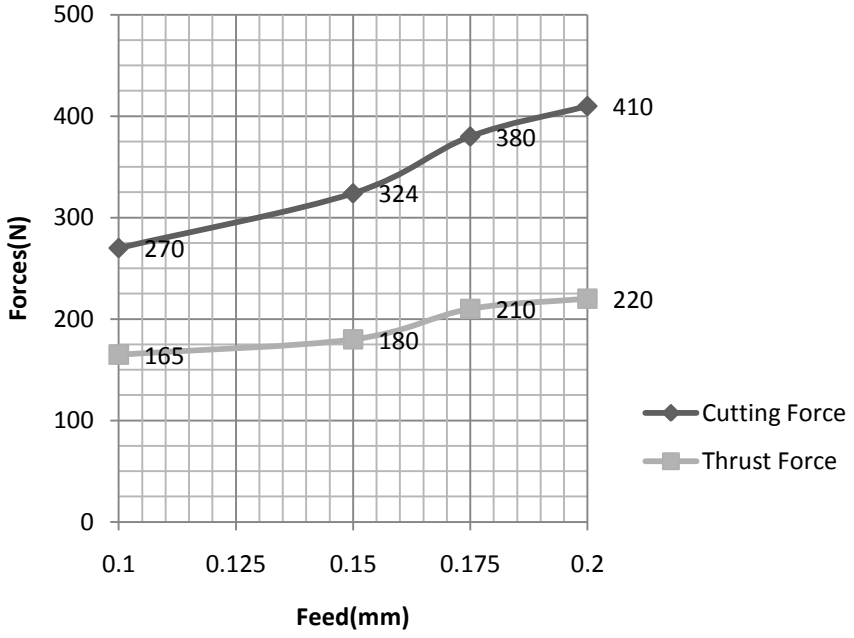

Figure 5.3: Measured forces Al 7075 15% Alumina

(Vc =60m/min; d=3mm; r_n=0 .4mm; r_e= 5μm) [17]

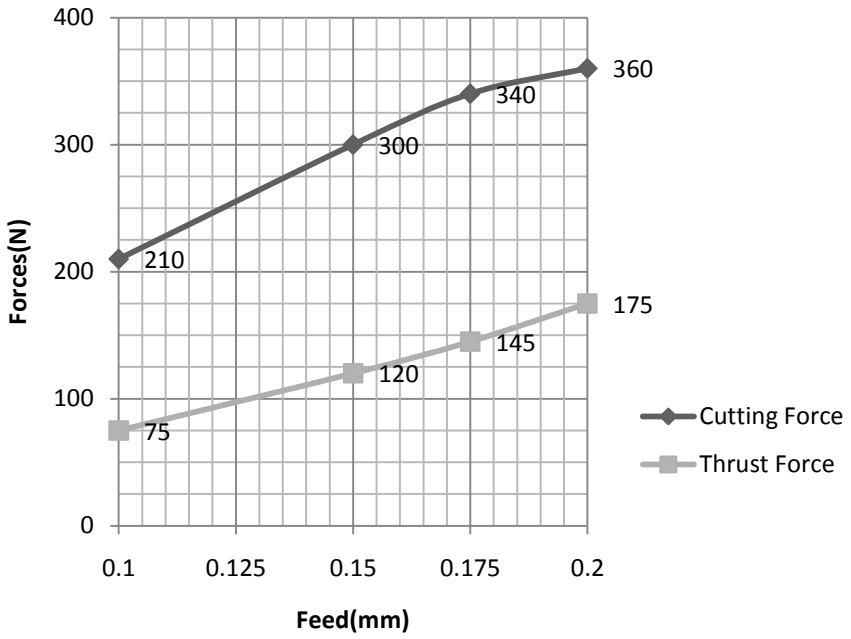

Figure 5.4: Measured forces Al 6061 10% Alumina,

(Vc =60m/min; d=3mm; r_n=0 .4mm; r_e= 5µm) [17]

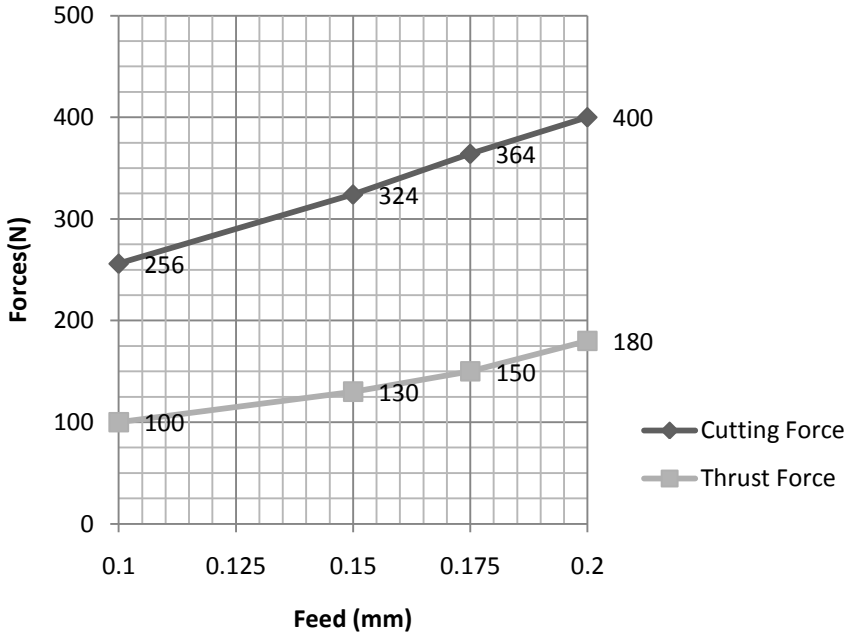

Figure 5.5: Measured forces Al 6061 20% Alumina

(Vc =60m/min; d=3mm; r_n=0 .4mm; r_e=5µm) [17]

5.4 Comparison of Predicted and Experimental Results

5.4.1 Mechanical Properties of the Composite Metal and Cutting Tool

Material and tool properties were obtained from the literature. The Johnson-Cook parameters for the two matrix materials are listed in Table 5.1. These material constants are used to calculate the constant k in Equation 4.3 and 4.4. The mechanical properties of hard ceramic Al_2O_3 , material matrix, and the cutting tool are listed in Table 5.2.

Table 5.1: The values of Johnson-Cook equation for these two Aluminum matrices [100]

Matrix	A	B	N	C	M	T_m
Al7075	496	310	0.3	0.0	1.2	635
Al6061	324	224	0.42	0.002	1.34	582

Table 5.2: Properties of hard ceramic tool, Al_2O_3, and material matrix [17,101]

	Young's Modulus (MPa)	Poisson Ratio	Hardness	Thermal Conductivity (W/m-K)
Al_2O_3	340	0.22		
Ceramic tool	420	0.2	21.58	
7075Al-15%	114	0.29		138
7075Al-10%	110	0.26		132
6061Al-20%	90	0.26		160
6061Al-10%	85	0.24		156

5.4.2 Comparison, Results and Discussions

Figure 5.6 represents the comparison between the predicted and experimentally measured cutting forces for 7075 Al MMC with 10 and 15% Alumina reinforcements. From the chart it can be found that the cutting forces are increasing with the increase in feed and prediction error is less than 3% shown in table 5.3. Moreover, the cutting forces are increasing with the increase of volume fraction of the reinforce particle which is due to increase in frictional force in chip-tool interface and the debonding force.

Figure 5.7 shows the comparison between the predicted and experimental value of cutting forces for 6061 Al MMC with 10 and 20% reinforcement particles. Prediction error in this case is less than 3% as well shown in table 5.3. The predictions revealed that, the force due to chip formation is much higher than those due to ploughing and the particle fracture. Generally it was about 98-95% of total force. For the 6061 -20 % alumina (*Vc =60m/min, d=3mm feed =0.15mm)* the shear angle is calculated as 17.94°. Total cutting force is calculated as 323N and measured cutting force was 324N. A good agreement between model and experiment can be seen.

Figure 5.8 and 5.9 shows the thrust forces for 6061-Al and 7075-Al MMC for different feed rates and reinforcements. It can be seen that the prediction error is within 10-20% range as shown in table 5.3. For the 6061-20 % alumina (*Vc =60m/min, d=3mm feed =0.15mm)* thrust force is calculated as 165 N and measured force is 180 N, which also proves good agreement between measured and predicted force

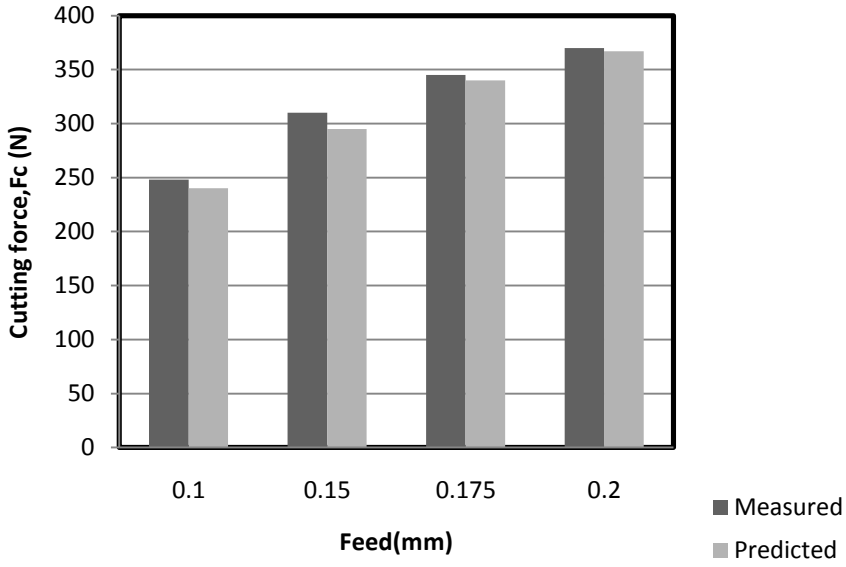

a) 10% Alumina reinforcement

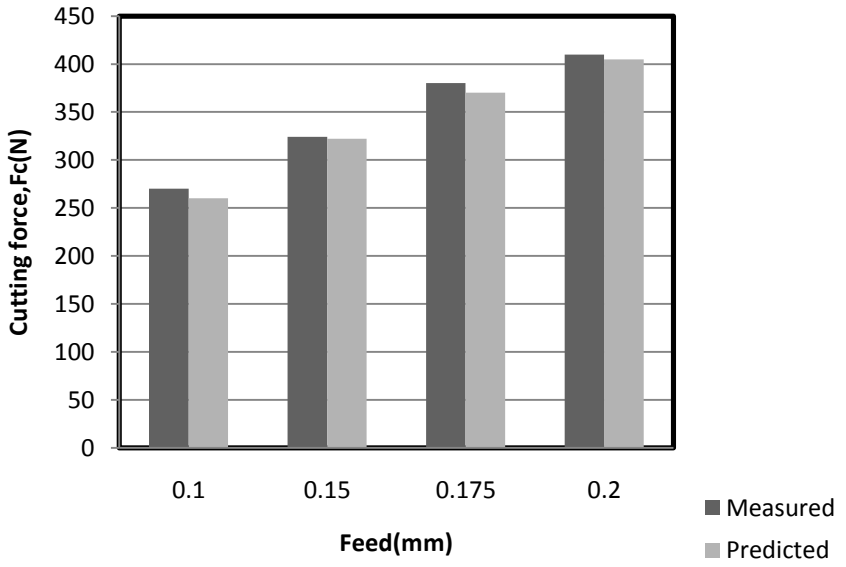

b) 15% Alumina reinforcement

Figure 5.6: Predicted Cutting force (Fc) when cutting 7075 aluminum base MMC (Vc =60m/min; d=3mm; r_n=0 .4mm; r_e= 5μm)

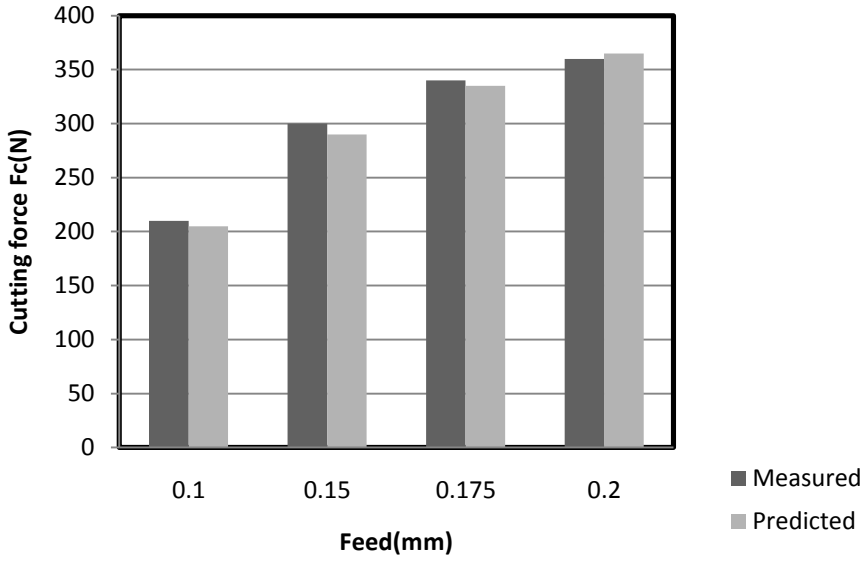

a) 10% Alumina reinforcement

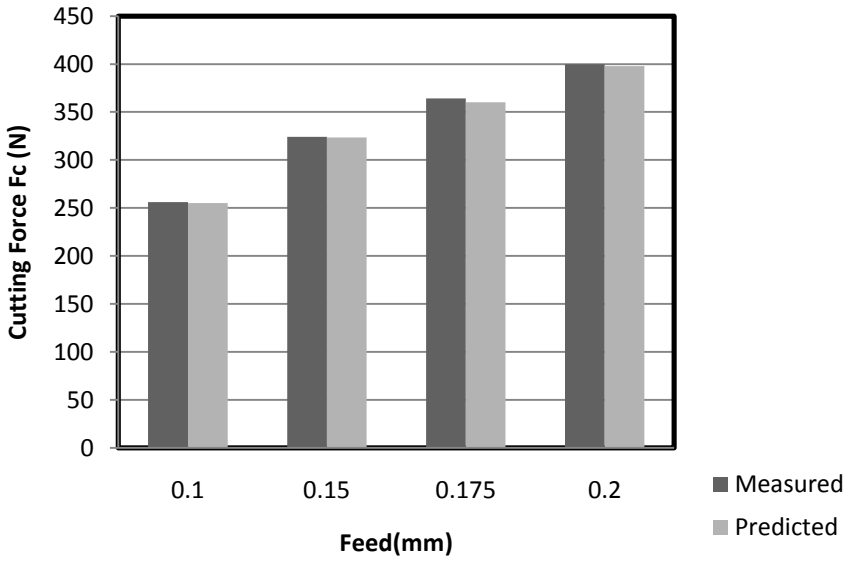

b) 20% Alumina reinforcement

Figure 5.7: Predicted Cutting force (Fc) when cutting 6061 aluminum base MMC (Vc =60m/min; d=3mm; r_n=0 .4mm; r_e=5µm)

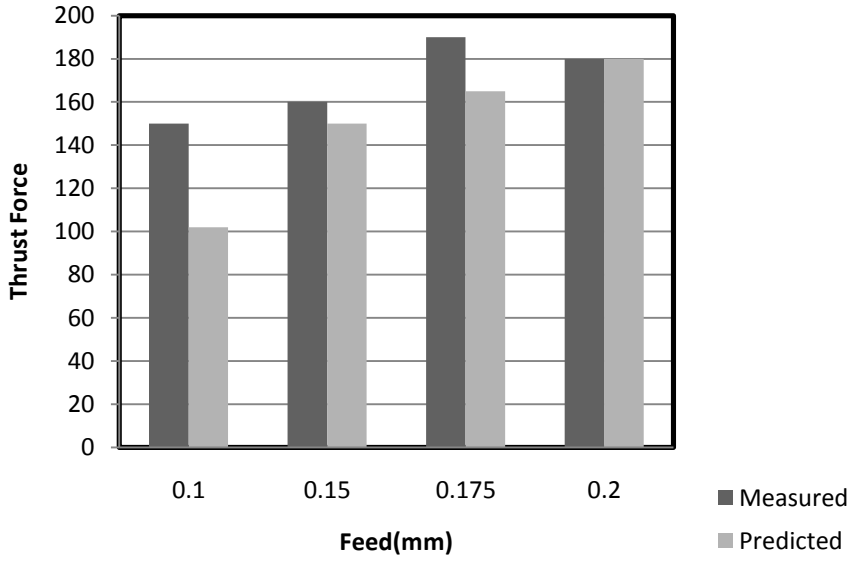

a) 10% Alumina reinforcement

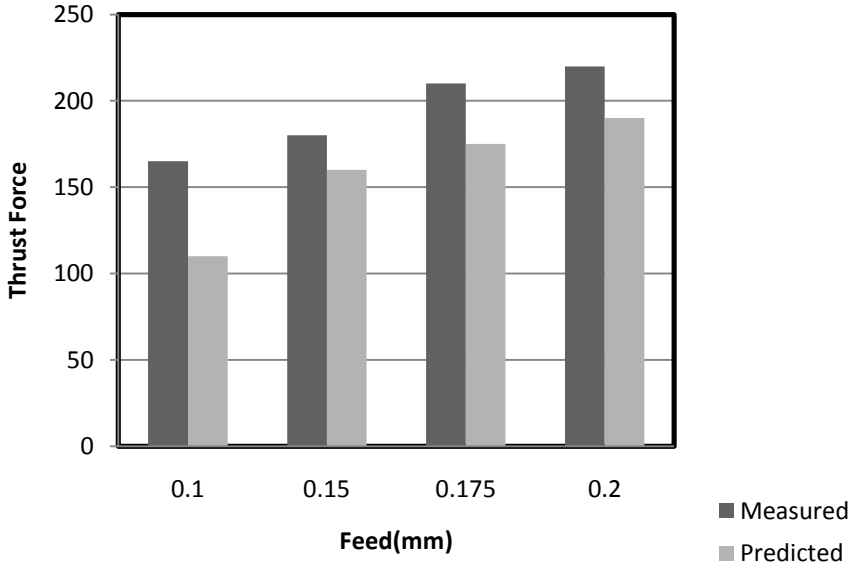

b) 15% Alumina reinforcement

Figure 5.8: Predicted thrust force (F_T) when cutting 7075 aluminum base MMC (Vc =60m/min; d=3mm; r_n=0 .4mm; r_e= 5µm)

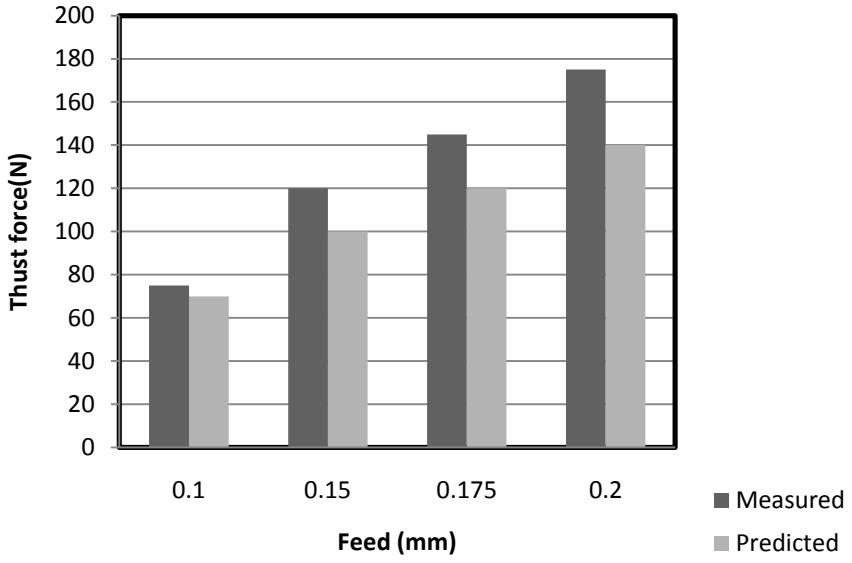

a) 10% Alumina reinforcement

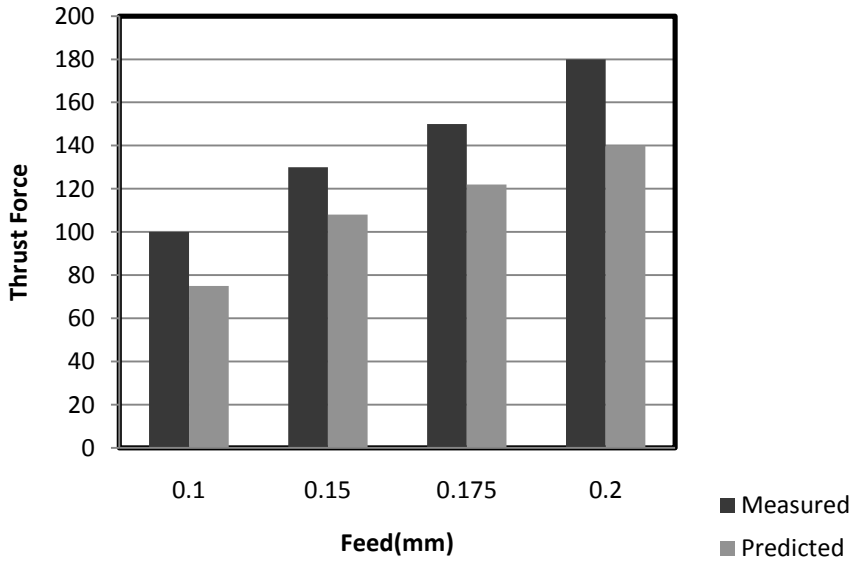

b) 20% Alumina reinforcement

Figure 5.9: Predicted thrust force (F_T) when cutting 6061 aluminum base MMC (Vc =60m/min; d=3mm;r_n=0 .4mm;r_e = 5μm)

Table 5.3: Prediction error for current model

Feed rate (mm)	7075 Al 10% Alumina MMC		7075 Al 15% Alumina MMC		6061 Al 10% Alumina MMC		6061 Al 20% Alumina MMC	
	Cutting direction	Thrust direction	Cutting direction	Thrust direction	Cutting direction	Thrust direction	Cutting direction	Thrust direction
0.1	2.9%	20%	2%	20%	1%	5%	.1%	15%
0.15	3%	5%	.5%	5.7%	1.7%	10%	.2%	12%
0.175	1.5%	7.5%	2.5%	8.5%	1.5%	12%	.5%	10%
0.2	.7%	.1%	1.7%	7.5%	1%	18%	1%	22%

From the data, it is also found that, soft matrix like 6061-Al MMC can be easily cut due to its low shear strength than 7075-Al MMCs. Ductility of the matrix protects the tool by pushing in the matrix or ploughing particle through the chip-tool interface. On the other hand, the friction force and the total cutting forces increase with the increase in the volume fraction and reinforcements particle size. As seen from the Figure 5.10, the amount of debonding energy is significantly increased with the increase in the particle size. This is because there is an increase in contact surface during debonding. The force for the debonding ceramic particles for the aluminum matrix in the MMC is much smaller than the force due to shearing of aluminum matrix.

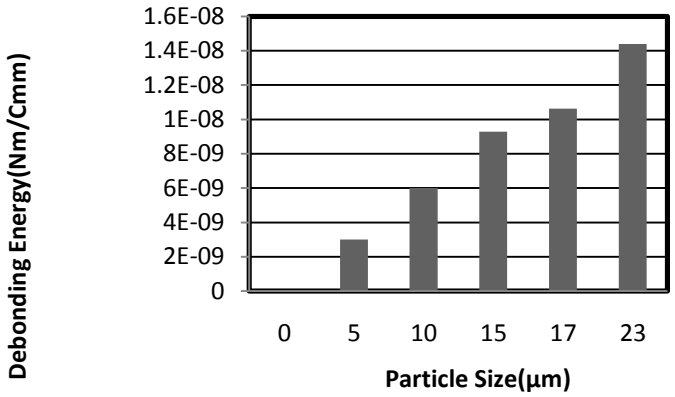

Figure 5.10: Debonding energy per particle with different alumina particle size

Figure 5.11 shows the predicted frictional forces along chip-tool interface for MMC 6061-Al-20% reinforcements, under different feed rates. Form the figure it was found that frictional forces are 20% of total forces in cutting direction. Compared to monometallic materials, the fractured particles of MMCs on the machined surface and chip-tool interface are the main sources for the increased cutting force, shortened tool lives, and sub-surface damage.

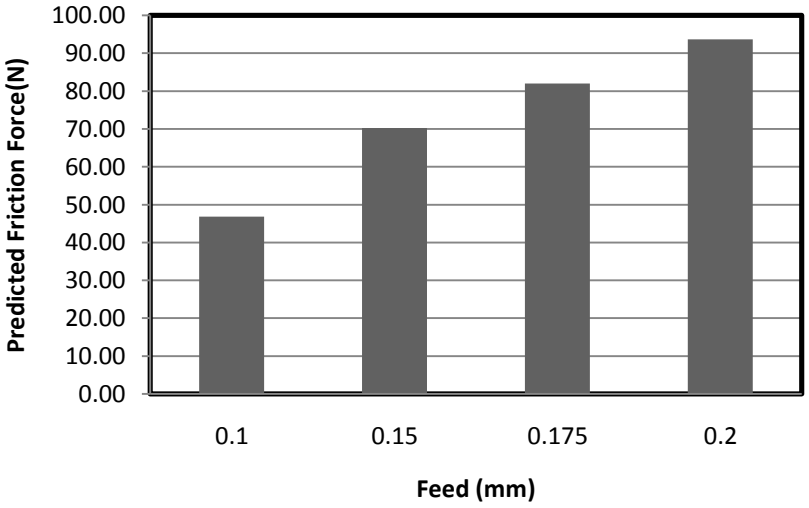

Figure 5.11: Chip- tool frictional force for 6061-20%

5.5 Summary

The predicted forces generated by using the force model showed good agreement with the experimentally measured forces and were with an average of 15% error. The predictions revealed that, the force due to chip formation is much higher than those due to ploughing and particle fracture. The model also predicted that debonding and particle fracture force is significantly increased with the increase in the particle size and chip thickness ratio is decreasing with the increase of the volume fraction of the reinforcement particle.

CHAPTER 6

CONCLUSIONS AND RECOMMENDATIONS

6.1 Summary

The primary aim of the research was to develop a force model to predict the generated forces during the machining metal matrix composites. In estimating the generated forces several aspects of cutting mechanics were considered, such as: shearing force, ploughing force, and particle fracture force. Shearing deformation force was obtained by analyzing the classical orthogonal metal cutting mechanics and Johnson-Cook equation. Ploughing force was formulated and fracture force was calculated based on the Griffith theory of failure. The predicted results and previously measured experimental data were compared under different cutting conditions such as speed, depth of cut, and feed rate.

6.2 Conclusions

The main conclusions of this work can be summarized as follows:

1. A model has been developed to predict cutting forces during machining of composites by incorporating the frictional characteristics at chip–tool and work–tool interfaces, ploughing force along the edge radius and particle fracture force.
2. The model predicts forces in the cutting direction with an error of 3% (or less) and cutting forces in thrust direction within 15% error.
3. The force due to chip formation is much higher than those due to ploughing and particle fracture.
4. The total cutting forces increase with the increase in the volume fraction and reinforcements particle size.
5. It was found that frictional forces in chip-tool interface are 20% of total forces in cutting direction.
6. Debonding and particle fracture force is significantly increased with the increase in the particle size.
7. Chip thickness ratio is decreasing with the increase of the volume fraction of the reinforcement particle.
8. The fractured reinforcement particles of MMCs on the machined surface and chip-tool interface are the main sources for the increased cutting forces, shortened tool lives and sub-surface damage.

6.3 Recommendation for Future Work

The following suggestions are made for the future investigation on force modeling in machining metal matrix composites:

1. Further exploration on reinforcement particle debonding, cracking and pull out from the metal matrix during machining metal matrix composites.
2. Accurate measurement of MMCs material properties such as flow stress, yield strength, conductivity and fracture strength under high strain rate are needed.
3. Effects of coolant during machining MMCs are needed to be studied.

References

[1] M.C. Shaw, *Metal Cutting Principles*, Oxford University Press, 1984.

[2] N. Chawla, K.K. Chawla, *Metal Matrix Composites*, Springer, New York, 2006.

[3] M.K. Surappa, Aluminum Matrix Composites-Challenges and opportunities, *Sadhana*, Vol.**28**, Parts 1& 2, (2003), pp. 319-324.

[4] A. Pramanik, L.C. Zhang, J.A. Arsecularatne, Prediction of cutting forces in machining of metal matrix composites, *International Journal of Machine Tools and Manufacture* **46** (2006), pp. 1795–1803.

[5] R. Teti, Machining of composite materials, *Annals of the CIRP* **51** (2002), pp. 611–634.

[6] T.W. Clyne, P.J. Withers, *An Introduction to Metal Matrix Composites*, Cambridge University Press, Cambridge (1993).

[7] W. Brown, W. Harrigan, J.F. Dolowy, *Proc. Verbundwerk 90*, Demat, Frankfurt (1990), pp. 20.1–20.15.

[8] *Manufacturers of Discontinuously Reinforced Aluminum (DRA)*, DWA Composite Specialities Inc., Chatsworth USA (1995).

[9] K.U. Kainer (Ed.), *Metallische Verbundwerkstoffe*, DGM Informationsgesellschaft, Oberursel (1994).

[10] A.G. Leatham, A. Ogilvy, L. Elias, The Osprey process current status and future possibilities, *Proceedings of International Conference on P/M in Aerospace, Defence, and Demanding Applications*, MPIF, Princeton, USA (1993), pp. 165–175.

[11] Material Manual, Cospray Ltd. Banbury, U.K., 1992.

[12] K.U. Kainer (Ed.), *Metal Matrix Composites*, *Custom-made Materials for Automotive and Aerospace Engineering*, Wiley-VCH, Weinheim, 2006.

[13] R.A. Schapery, Thermal expansion coefficients of composite materials based on energy principles, *Journal of Composite Materials* **23** (1968), pp.380–404.

[14] W.H. Hunt Jr., T.M. Osman, J.J. Lewandowski, J. Masenvue, Fabrication of Particulate Reinforced Metal Matrix Composites, *ASM International Conference, Berlin* (1990).

[15] N.C. Beck, RM. Aikin Jr., R.M. Briber, Fracture Toughness of Discontinuously Reinforced Al-4Cu-1.5Mg/TiB Composites, *Metallurgical and Materials Transactions* **25** 11, pp. 2461-2468.

[16] N. Chawla, K.K. Chawla, Microstructure Based Modeling of the Deformation Behavior of Particle Reinforced Metal Matrix Composites, *Journal of Material Scence* **41** (2006), pp. 913-925.

[17] S. Kannan, Machining of metal matrix composites: forces, tool wear, attainable surface quality, *PhD Thesis* (2006).

[18] I. Finni, Review of the Metal Cutting Theories of the Past Hundred Years, *ASME Mechanical Engineering* **78** (1956), pp. 715-721.

[19] D. Stephenson, J. Agapiou, *Metal Cutting Theory and Practice*, second Ed, Marcel Dekker Inc, New York, USA, ISBN 0-8247-5888-9, 1997.

[20] N.N. Zorev, *Metal Cutting Mechanics*, Pergamon Press, 1966.

[21] M. Cocquilhat, Expériences sur la Resistance utile produites dans le Forage, *Annals des Travaux Publics en Belgique* **10** (1851), pp. 199.

[22] E. Hartig, B.G. Teubner, *Versuche über leistung und arbeits-verbrauch der werkzeugmaschinen*, Leipzig, 1873.

[23] I.A. Time, *Resistance of Metal and Wood to Cutting* (Soprotivleniye Metallov i Dereva Rezaniyu), 1870.

[24] H. Tresca, Mémories sur le rabotage des métaux, *Bulletin de la Société d'Encouragement pour l'Industrie Nationale* (1873), pp. 587–685.

[25] A. Mallock, The action of cutting tools, *Proceedings of the Royal Society XXXIII* (1881), pp. 127–139.

[26] L.N. Payton, A Correction to the 20th Century Orthogonal Metal Cutting, *Proceedings of the 2009 Industrial Engineering Research Conference(2009*).

[27] H. Ernst, Physics of Metal Cutting, *ASME Conference, Cleveland, OH*, 1938.

[28] V. Piispanen, Theory of formation of metal chips, *Journal of Applied Physics* **19** (1948), pp. 877–881.

[29] M.E. Merchant, Basic mechanics of the metal cutting process, *Transactions of ASME* **66** (1944), pp. A65–A71.

[30] K. J. Trigger, B.T. Chao, An analytical evaluation of metal cutting temperature, *Transactions of ASME* **73** (1951), pp. 57–68.

[31] E.G. Loewen, M.C. Shaw, On the analysis of cutting tool temperatures, *Transactions of ASME* **71** (1954), pp. 217–231.

[32] W.A. Marcos, A slip line field solution of the free continuous cutting problem in conditions of light friction at chip–tool interface, *Journal of Engineering for Industry* **102** (1980), pp. 310–314.

[33] P.K. Venuvinod , W.L. Jin, Three Dimensional Cutting Force Analysis Based on the Lower Boundary of the Shear Zone, Part I: Single Edge Oblique Cutting, Part II: Two Edge Oblique Cutting, *International Journal of Machine Tools and Manufacture* **36** (3) (1996), pp. 307–338.

[34] C.A. Van Luttervelt, T.H.C. Childs, I.S. Jawahir, F. Klocke, P.K. Venuvinod, Present Situation and Future Trends in Modelling of Machining Operations, *Annals of the CIRP* **48** (2) (1998), pp. 587–626.

[35] S.P.F.C. Jaspers, Metal cutting mechanics and material behaviour, *Ph.D. Thesis, Eindhoven University of Technology*, (1999).

[36] G.C.I. Lin, P. Mathew, P.L.B. Oxley, A.R. Watson, Predicting cutting forces for oblique machining conditions, *Proceedings of the Institute of Mechanical Engineers* **196** (1982), pp. 141–148.

[37] N.H. Cook, I. Finnie, M.C. Shaw, Discontinuous Chip Formation, *Transactions of ASME*. **76** (1954), pp. 153–162.

[38] R. Komanduri, R.H. Brown, The mechanics of chip segmentation in machining, *Transactions of American Society of Mechanical Engineers Journal of Engineering for Industry* **103** (1981) (1), pp. 33–51.

[39] K.F. Sullivan, P.K. Wright, P.D. Smith, *Metallurgical appraisal of instabilities arising in machining, Metals Technology* **5** (1978), pp. 181.

[40] L.V. Colwell, Predicting the Angle of Chip Flow for Single-Point Cutting Tools, *Transactions of ASME, **76*** 2 (1954), pp. 199–204.

[41] M.C. Shaw, N.H. Cook, P.A. Smith, The mechanics of three-dimensional cutting operations, *Transactions of ASME* **74** (1952), pp. 1055.

[42] G.V. Stabler, The foundational geometry of cutting tool, *Institution of Mechanical Engineers - Proceedings* **165** (1951), pp. 14-21.

[43] G.R. Johnson, W.H. Cook, A constitutive model and data for metals subjected to large strains, high strain rates and high temperatures, *Proceedings of the 7thInternational Symposium on Ballistics, The Hague, Netherlands* (1983), pp. 541–547.

[44] H. Ernst, M.E. Merchant, Chip formation friction and high quality machined surfaces, Surface Treatment of Metals, *ASM, New York* (1941).

[45] E.H. Lee, B.W. Shaffer, The theory of plasticity applied to a problem of machining, *ASME Journal of Applied Mechanics.* **18** (1951), pp. 405–413.

[46] S. Kobayashi, E.G. Thomsen, The role of friction in metal cutting, *Journal of Engineering for Indndustry* **82** (1960), pp. 324.

[47] M.C. Shaw, N.H. Cook, I. Finnie, The shear-angle relationship in metal cutting, *Transactions of ASME* **75** (1953), pp. 273.

[48] H. Hucks, Dissertation, *Aachen*, 1951.

[49] E. Shamoto, Y. Altintas, Prediction of shear angle in oblique cutting with maximum shear stress and minimum energy principles, *Transactions of ASME, Journal of Manufacturing Science and Engineering,* **121** (1999), pp. 399-407.

[50] R. Komanduri, Machining and Grinding - A Historical Review of the Classical Papers, *ASME Applied Mechanics Review* **46** (1993), pp. 80–132.

[51] K. Okushima, K. Hitomi, An analysis of the mechanism of orthogonal cutting and its application to discontinuous chip formation, *ASME Journal of Engineering for Industry* **8** (1961), pp. 545.

[52] N.N. Zorev, Inter relationship between shear processes occurring along tool face and on shear plane in metal cutting, *International Research in Production Engineering Proceedings of the International Production Research Conference, Carnegie Institute of Technology, Pittsburg, PA* (1963), pp. 3–17.

[53] P.L.B. Oxley, M.J.M. Welsh, Calculating the shear angle in orthogonal metal cutting from fundamental stress, strain, strain-rate properties of the work material, *Proceedings of the 4th International Machine Tool Design and Research Conference, Pergamon, Oxford* (1963), pp. 73–86.

[54] E. Usui, A. Hirota, M. Masuko, Analytical prediction of three dimensional cutting process, Part 1, Basic cutting model and energy approach, *ASME Journal of Engineering for Industry* **100** (2) (1978), pp. 222.

[55] D.W. Wu, A New Approach of Formulating the Transfer Function of Dynamic Cutting Processes, *Journal of Engineering for Industry* **111**(11) (1989), pp.37-47.

[56] M.A. Elbestawi, F. Ismail, R. Du, B.C. Ullagaddi, *Winter Annual Meeting Atlanta, ASME Publication PED* **54** (1991), pp. 253.

[57] W.J. Endres, D.J. Waldorf, The importance of considering size effect along the cutting edge in predicting the effective lead angle for turning, *Transactions of NAMRI/SME* **22** (1994), pp. 65–72.

[58] Y. Zhu, On Machining Metal Matrix Composites: A Finite element Model, *MASc Thesis* **2** (2004), pp. 32-34.

[59] ABAQUS, Theory Manual and User's Manuals, Version 6.2.

[60] A.O. Tay, M.G. Stevenson, G. Devahl Davis, Using the finite element method to determine temperature distributions in orthogonal machining, *Proceedings of the Institution of Mechanical Engineers* **188** (1984), pp. 627.

[61] F.P. Bowden, D. Tabor, *Friction and Lubrication of Solids Part II*, Oxford Univ. Press, Clarendon Press, London, 1964.

[62] E. Usui, H. Takayama, The effect of tool chip area in metal cutting, *Transaction of ASME*, **80** (1958), pp. 1089.

[63] D.J Waldorf, A simplified model for ploughing forces in turning, *Transaction of NAMRI of SME* **32** (2004), pp. 447–454.

[64] H. Hocheng, S.B. Yen, T. Ishihara, B.K. Yen, Fundamental turning characteristics of a tribology-favored graphite/aluminum alloy composite material , 2 May (1997).

[65] S. Kannan, H.A. Kishawy, M. Balazinski, An energy based analytical force model for orthogonal cutting of metal matrix composites, *Annals of the CIRP* **53** (1) (2004), pp. 91–94.

[66] U. Dabade, D. Dapkekar, S.S. Joshi, Modeling of Chip-tool interface friction to predict cutting forces in machining of Al/SiCp composites, *International Journal of Machine Tools and Manufacture* **49** (2009), pp. 690-700.

[67] N.P. Hung, S. Jana, L.J. Yang, C.H. Heng, Laser drilling of cast metal matrix composites , *Proceedings on Machining of Advanced Materials ASME AMD, Los Angeles* **1** 208 (1995), pp. 87-92.

[68] N. Tomac, K. Tonnessen, Machinability of paniculate aluminium matrix composites, *Annals of the CIRP* **41/1** (1992), pp. 55-58.

[69] K. Weinert, W. König, A consideration of tool wear mechanisms when machining metal matrix composites (MMC), *Annals of the CIRP* **42** (1) (1993), pp. 95–98.

[70] N.P. Hung, F.Y.C. Boey, K.A. Khor, Y.S. Phua, H.F. Lee, Machinability of aluminum alloys reinforced with silicon carbide particulates, *International Conference on Advances in Material and Processing Technologies* (1993), pp. 9–20.

[71] C.T. Lane, Machining characteristics of particulate-reinforced aluminium, Fabrication of Particulates Reinforced Metal Composites, *ASM* (1990), pp.195.

[72] J.T. Lin, D. Bhattacharyya, C. Lane, Machinability of a silicon carbide reinforced aluminum metal matrix composite, *Wear* **181** (1995), pp. 883–888.

[73] K. Weinert, A consideration of tool wear mechanism when machining metal matrix composites (MMC), *Annals of CIRP* **42** 1 (1993).

[74] C.J.E. Andrewes, H.Y. Feng, W.M. Lau, Machining of an aluminum/SiC composite using diamond inserts, *Journal of Materials Processing Technology* **102** (2000), pp. 25-29.

[75] M. El-Gallab, M. Sklad, Machining of Al-SiC particulate metal-matrix composites. Part I: tool performance, *Journal of Materials Processing Technology* **83** (1998), pp. 151–158.

[76] S. Barnes, I.R Pashby, K. Mok, The effect of workpiece temperature on the machinability of an aluminum/ SiC MMC, *Transactions of ASME, Journal of Manuf. Sci. Eng*. **118** (1996), pp. 422–427.

[77] A. Pramanik, L.C. Zhang, J.A. Arsecularatne, An FEM investigation into the behavior of metal matrix composites: tool- particle interaction during orthogonal

cutting. *International Journal of Machine Tools and Manufacture* **47** (2007), pp. 1497–1506.

[78] N.P. Hung, V.C. Venkatesh, N.L. Loh, Cutting Tools for Metal Matrix Composites, *Key Engineering Materials*, **138** 140 (1998), pp. 289-325.

[79] N.P. Hung, Z.W. Zhong, C.H. Zhong, Grinding of Metal Matrix Composites Reinforced with Silicon-Carbide Particles, *Journal of Materials and Manufacturing Processes* **12** (6) (1997), pp. 1075-1091.

[80] Songmene, M. Balazinski, Machinability of Graphitic Metal Matrix Composites as a Function of Reinforcing Particles, *Annals of the CIRP* **48/1** (1999), pp. 77–80.

[81] R.S. Lee, G.A. Chen, B.H. Hwang, Thermal and grinding induced residual stresses in a silicon-carbide particle-reinforced aluminum metal matrix composite, *Composites* **26** 6 (1995).

[82] C.T. Lane, Drilling and tapping of SiC reinforced Al, *Proceedings of the Machining of Composite Materials Conference, ASM International, Pittsburgh, PA. Monaghan* (1993).

[83] A. Paoletti, A. Di Ilio, V. Tagliaferri, F. Veniali, An experimental study on grinding of silicon carbide reinforced aluminum alloys, *International Journal of Machine Tools and Manufacture* **36** 6 (1996), 673–685.

[84] A. Allen, M. Bourke, S. Dawes, M. Hutchings, P. Withers, *Acta Metall Mater.* **40** (1992), pp. 2361.

[85] J. Monaghan, P. O'Reilly, The drilling of an Al/SiC metal-matrix composite, *Journal of Materials Processing Technology* **33** (1992), pp. 469.

[86] N.P. Hung, S.H. Yeo, B.E. Oon, Effect of cutting fluid on the machinability of metal matrix composites, *Journal of Materials Processing Technology* **67** (2001), pp. 157–161.

[87] L. Cronjäger, D. Meister, Machining of fibre and particle-reinforced aluminum MMC, *CIRP* **41** 1 (1992), pp.63–66.

[88] S. Barnes, I.R. Pashby, Through-Tool Coolant Drilling of Aluminum/SiC Metal Matrix Composite, *ASME Journal of Materials Processing Technology* **122** 4 (2000), pp. 384–388.

[89] R. Shetty, R.B. Pai, S.S. Rao, B.S. Shenoy, Study of tool wear in turning 15% SiCp reinforced 6061 aluminum metal matrix composite with steam as coolant, *Proceedings of International conference on Advanced Material processing and characterization* (2010).

[90] N.P. Hun, S.H. Yeo, K.K. Lee, K.J. Ng, Chip formation in machining particle-reinforced metal matrix composites, *Materials and Manufacturing Processes* **13** (1) (1998), pp.85–100.

[91] J.T. Lin, D. Bhattacharyya, W.G. Ferguson, Chip formation in the machining of SiC-particle-reinforced aluminum-matrix composites, *Composites Science and Technology* **58** (1998), pp. 285–291.

[92] P.L.B. Oxley, *Mechanics of Machining: An Analytical Approach to Assessing Machinability*, first ed., Wiley, New York, 1989.

[93] M. Kronenberg, *Machining Science and Application*, first English ed., Pergamon Press, Great Britain, 1966, pp. 53.

[94] L.V. Colwell, Predicting the angle of chip flow for single-point cutting tool, *Transaction of ASME* **76** (1954), pp. 199–204.

[95] Y. Sahin, G. Sur, The effect of Al2O3, TiN and TiC, N-based CVD coatings on tool wear in machining metal matrix composites, *Surface and Coatings Technology* **179** (2004), pp. 349–355.

[96] L. Xiaoping, W.K.H. Seah, Tool wear acceleration in relation to workpiece reinforcement percentage in cutting of metal matrix composites, *Wear* **247** (2001), pp. 161–171.

[97] J. Jiaren, S. Fanghui, R. Fengshen, Modeling of two body abrasive wear under multiple contact conditions, *Wear* **217** (1998), pp.35–45.

[98] S. Venkatachalam, S. Liang, Effects of ploughing forces and friction coefficient in micro-scale machining, *Transactions of ASME, Journal of Manufacturing Science and Engineering* **129** (2007), pp. 274–279.

[99] H. Sin, N. Saka, N.P. Suh, Abrasive wear mechanisms and the grit size effect, *Wear* **55** (1979), pp. 163–190.

[100] N. Fang, A new quantitative sensitivity analysis of the flow stress of 18 Engineering materials in machining, *Transactions of ASME, Journal of Engineering Materials and Technology* **127** (2005), pp. 192–196.

[101] E.D. Whitney, *Ceramic cutting tools: materials, development, and performance*, Noyes Publication, 1994.